



저작자표시-비영리-동일조건변경허락 2.0 대한민국

이용자는 아래의 조건을 따르는 경우에 한하여 자유롭게

- 이 저작물을 복제, 배포, 전송, 전시, 공연 및 방송할 수 있습니다.
- 이차적 저작물을 작성할 수 있습니다.

다음과 같은 조건을 따라야 합니다:



저작자표시. 귀하는 원저작자를 표시하여야 합니다.



비영리. 귀하는 이 저작물을 영리 목적으로 이용할 수 없습니다.



동일조건변경허락. 귀하가 이 저작물을 개작, 변형 또는 가공했을 경우에는, 이 저작물과 동일한 이용허락조건하에서만 배포할 수 있습니다.

- 귀하는, 이 저작물의 재이용이나 배포의 경우, 이 저작물에 적용된 이용허락조건을 명확하게 나타내어야 합니다.
- 저작권자로부터 별도의 허가를 받으면 이러한 조건들은 적용되지 않습니다.

저작권법에 따른 이용자의 권리는 위의 내용에 의하여 영향을 받지 않습니다.

이것은 [이용허락규약\(Legal Code\)](#)을 이해하기 쉽게 요약한 것입니다.

[Disclaimer](#)

공학박사학위논문

**Synthesis of VO₂ nanowire and fabrication
nanodevices based on metal-to-insulator
transition of VO₂**

이산화바나듐 나노와이어의 합성과 금속-절연체
상전이를 이용한 나노소자 개발 연구

2014년 2월

서울대학교 대학원

재료공학부

배 성 환

Abstract

Synthesis of VO₂ nanowire and fabrication nanodevices based on metal-to-insulator transition of VO₂

Sung-Hwan Bae

Department of Materials Science and Engineering

The Graduate School

Seoul National University

Vanadium dioxide (VO₂) nanowire was synthesized by hydrothermal process which was followed by thermal annealing in order to fabricate the devices and investigate the applicability of the devices which are based on metal-to-insulator transition.

First, the hydrothermal process was performed with various conditions in order to investigate the effect of process time and temperature on the structure of the VO₂

nanowire. The VO₂ hydrate nanowires were formed after hydrating–exfoliating–splitting steps through the hydrothermal process, and each step was confirmed by the field emission scanning electron microscope (FESEM). As the process temperature increased, the nanowire became thinner. As the process time increased, the nanowire became thinner, but the limit of a convergent of the diameter was about 60nm. In order to dehydrate the nanowires, thermal annealing at 400°C in N₂ atmosphere for 4 hours was carried out. XRD and DSC results showed that the nanowires were VO₂(M) without any hydrate phases and that the MIT occurred at ~68°C in a heating cycle. These results suggest that the new method to synthesize the pure VO₂(M) nanowires.

Second, in order to investigate the memristive properties of the VO₂ nanowire, the VO₂ nanowire was connected electrically by using silver contact. The MIT of a single VO₂ nanowire can be successfully controlled by self-Joule heating without additional heating source. Non-volatile resistive memory can be stabilized by bias voltage to read the resistance. Various resistance states can be achieved due to the controlled formation and growth of metallic clusters on micrometric regions by efficient Joule heating that accompany with voltage pulse. The process of writing with voltage pulse and erasing with thermal cooling shows very high reproducibility in resistance. The VO₂ nanowire can be non-volatile resistive memory can be stabilized by bias voltage to read the resistance. Various resistance

states can be achieved due to the controlled formation and growth of metallic clusters on micrometric regions by efficient Joule heating that accompany with voltage pulse.

Third, the effect of pressure on memritive properties of the single VO₂ nanowire was investigated for gas sensor application. The MIT of a single VO₂ nanowire can be successfully controlled by self-Joule heating without additional heating source. Non-volatile resistive memory can be stabilized by bias voltage which can be determined from the transition voltage in I-V curve. When same voltage pulse applied to the nanowire, as the pressure decreased, the resistances of nanowire change more lower value in mixed state.

Finally, in order to investigate the thermochromic properties of the VO₂ nanowire, VO₂ and polymer composites were deposited on fused silica substrate by the spin coating method. Colloidal VO₂ nanowires are fundamental materials of thermochromic coatings. After (3-methacryloxypropyl)trimethoxysilane(MPTMS) treatment, VO₂ nanowires were dispersed in 2-butanone, forming a visually transparent colloid. VO₂ nanowire-SiO₂ core-shell nanostructure was fabricated by the silanization via hydrolysis of TEOS for antireflection coating. The micro and nano-structure of VO₂ nanowire-SiO₂ core-shell was investigated by the microscope, the FESEM and the TEM. As result of XRD and EDS, SiO₂ coating layer which has the thickness from 100nm to 100um was the amorphous silicon

oxide. Colloid VO₂ nanowire and VO₂-SiO₂ core-shell nanowires were dispersed in polyurethane and were deposited on fused silica substrate by the spin coating method. The thermochromic property was improved after MPTMS treatment and the transmittance in visible light was improved after SiO₂ antireflection coating.

Keywords: Vanadium oxide, Nanowire, Memristor, Gas sensor, Thermochromic coatings, Thermochromism, Metal-insulator transition, Hydrothermal process, Microstructure, Nanostructure, Post annealing,

Student Number: 2006-20849

Table of Contents

List of Figures.....	viii
List of Tables	xiii
Chapter 1. General Introduction.....	1
1.1 References.....	5
Chapter 2. General background.....	9
2.1 Vanadium dioxide(VO_2)	9
2.2 VO_2 nanodevice.....	13
2.3 Thermochromic Window based on VO_2	14
2.4 Vanadium dioxide nanowire	16
2.5 References.....	23
Chapter 3. Synthesis and properties of VO_2 nanowire	30
3.1 Hydrate VO_2 nanowire synthesis	30
3.2 Dehydrating process: post annealing process	35
3.3 Metal-to-insulating transition properties of VO_2 nanowire	37
3.4 References.....	39

Chapter 4. The memristive properties of a single VO₂ nanowire with switching controlled by self heating	41
4.1 Introduction.....	41
4.2 Experimental procedure.....	44
4.3 Results and discussions.....	45
4.4 Summary.....	59
4.5 Rerences.....	61
Chapter 5. Thermochromic properties of VO₂ and polymer composite for smart window application	66
5.1 Introduction.....	66
5.2 Experimental procedure.....	71
5.3 Results and discussions.....	72
5.4 Summary.....	76
5.5 References.....	77
Chapter 6. Thermochromic properties of VO₂ and polymer composite for smart window application	80
6.1 Introduction.....	80
6.2 Experimental procedure.....	86
6.3 Results and discussions.....	90
6.4 Summary.....	103

6.5 References.....	104
Chapter 7. Summary and suggestions for future work	106
Publications	111
Abstract in Korean	115

List of Figures

Figure 1-1 The flow chart of the rest chapter of this thesis	4
Figure 2-1 Conductivity as a function of reciprocal temperature for the lower oxides of titanium and vanadium.....	18
Figure 2-2 Schematic illustration of lattice of the two structural phases of VO ₂	19
Figure 2-3 Phase diagram for the vanadium-oxygen system	20
Figure 2-4 MIT-triggering approaches in correlated oxides. (i) Temperature-triggered MIT in VO ₂ . (ii) Electrically triggered MIT in Pr _{0.7} Ca _{0.3} MnO ₃ . (iii) Optically triggered MIT in Pr _{0.7} Ca _{0.3} MnO ₃ . (iv) Magnetically triggered MIT in Pr _{0.7} Ca _{0.3} MnO ₃ . (v) Strain/stress effects on MIT in VO ₂	21
Figure 3-1 Schematic of the hydrating–exfoliating–splitting model and FESEM images.....	33
Figure 3-2 FESEM images of nanowires which were carried out hydrothermal process for various temperature from 180 to 220 °C for 3 days.....	34
Figure 3-3 XRD (a) and TGA (b) result of VO ₂ hydrate nanowire and VO ₂ nanowire after annealing process.....	36

Figure 3-4 Differential scanning calorimetry (DSC) results of annealed VO₂ nanowires..... 38

Figure 4-1 FESEM image of a single VO₂ nanowire and silver contact. Resistance with bias voltage of annealed VO₂ nanowires at room temperature (triangle), at 100 °C (circle), and an as-synthesized nanowire at room temperature (square)... 53

Figure 4-2 The resistance–voltage (R–V) hysteresis curve. Insets show the crystal structures of VO₂ (M) and VO₂ (R). Schematics showing the gradual change of phases inside the nanowire at different points marked in the R–V curve. Black and white parts denote the metallic and insulating phase of nanowire, respectively, and the mixed state shows the presence of multiple resistance of VO₂ nanowire 54

Figure 4-3 Schematic of these two kinds of voltage and explanations about the roles of each voltage; the bias voltage used for monitoring the resistance could be a roll as heating stage, the voltage pulse could trigger the MIT and switch the resistance..... 55

Figure 4-4 Resistance of annealed VO₂ nanowires at room temperature with 0.3 V voltage bias. The 30 V (diamond), 20 V (triangle), and 10 V voltage pulses (circle) are applied for 0.25 seconds. Inset graph shows the change of resistance for 5 minutes with 0.3 V voltage bias and 20 V voltage pulse 56

Figure 4-5 The change of resistance measured with the amount (1, 3, 5, and 10 V) and the number (up to 10 times) of voltage pulses of a single VO ₂ nanowire. The well-defined multiple resistance values with large range can be obtained by controlling the amount and the number of voltage pulse.....	57
Figure 4-6 Demonstration of the information storage that shows reliable and non-volatile switching property of VO ₂ single nanowire. The 0.3 V voltage bias is applied for reading, and the 3 and 5 V voltage pulses are applied for writing. The zero voltage is used for erasing and resetting to initial resistance	58
Figure 5-1 The different operation systems between the VO ₂ gas sensor and the memristive gas sensor.....	70
Figure 5-2 Resistance with bias voltage of annealed VO ₂ nanowires in 760Torr (square), in 1Torr (circle), and in 40mTorr (triangle)	74
Figure 5-3 The change of resistance measured with 2V voltage pulses of a single VO ₂ nanowire in 760Torr and 1Torr	75
Figure 6-1 ThermoSEE thermotropic glazing. The off-state is shown on the left and the heated on-state is shown on the right	83
Figure 6-2 Schematic illustration of thermochromic smart window.....	84
Figure 6-3 The step-by-step process of MPTMS treatment for dispersion.....	88

Figure 6-4 The step-by-step process of TEOS treatment to synthesize the VO ₂ -SiO ₂ core-shell nanowire	89
Figure 6-5 XRD diffraction pattern of VO ₂ -SiO ₂ core-shell nanowire (t=5min)	93
Figure 6-6 XRD diffraction pattern of VO ₂ -SiO ₂ core-shell nanowire (t=30min)	94
Figure 6-7 DSC results of the pure VO ₂ nanowire and VO ₂ -SiO ₂ core-shell nanowire	95
Figure 6-8 The microscope images of VO ₂ -SiO ₂ core-shell nanowires which are followed the reaction; t = 5min and	96
Figure 6-9 The graph and table which can show relationship between the reaction time and the	97
Figure 6-10 The actual nano-structure of VO ₂ -SiO ₂ core-shell nanowire was confirmed by TEM analysis.....	98
Figure 6-11 EDS mapping result of the VO ₂ -SiO ₂ core-shell nanowire successively synthesized.....	99
Figure 6-12 EDS mapping result of the VO ₂ -SiO ₂ core-shell nanowire successively	

synthesized..... 100

Figure 6-13 The spectral transmittance of VO₂ nanowire + polyurethane composite deposited on fused silica..... 101

Figure 7-1 The strategy of this thesis to fabricate the nanodevices based on VO₂ nanowire 110

List of Tables

Table 2-1 VO ₂ nano-devices.....	22
Table 5-1 Gas sensor performance of some 1-D oxide gas sensor.....	69
Table 6-1 Comparison of various smart windows.....	85

Chapter 1. General Introduction

Vanadium dioxide(VO_2) has been one of the most extensively studied material that shows a metallic-to-insulating phase transition since the first report in 1959 by E.J. Morin^[1]. It is well-known that VO_2 shows first-order phase transition at a certain critical temperature(T_c)^[2]. At temperature higher than the critical temperature T_c which is 340K, VO_2 is tetragonal-rutile structure($\text{VO}_2(\text{R})$) with high electrical conductivity, while below T_c , VO_2 is monoclinic structure ($\text{VO}_2(\text{M})$) with electrical insulating property. Through this reversible metal-to-insulator transition(MIT) near room temperature, VO_2 shows abrupt change in conductivity over three orders of magnitude.

VO_2 also undergoes an ultrafast ($\sim 10^2$ femtoseconds) transition when excited by a laser, and it shows metallic behavior under application of high electric-field ($\sim 10^6$ V/cm).^[3,4,5] This first-order MIT of VO_2 near room temperature has been widely studied over the last fifty years, yet the physics behind this intriguing phenomenon is not fully understood. The characteristics associated with MIT in VO_2 are

fascinating scientifically, letting VO₂ to have immense technological importance for potential applications in thermochromic windows, sensor and memory type applications.^[6,7,8,9]

Nanoscale materials often exhibit physical and chemical properties that differ from their bulk properties, and have attracted much attention because of their structural, electronic, and optical properties and their potential applications.^[10,11,12]

One-dimensional (1D) nanostructures include nanotubes, nanorods, nanowires, nanofibers, nanobelts, and nanoribbons. The 1D structural VO₂ materials lead to a wide variety of potential applications including lithium batteries temperature-sensing devices, optical switching devices, and thermochromic smart window.^[13,14,15,16,17,18,19,20]

Various deposition methods such as magnetron sputtering^[21,22], pulsed laser deposition^[23,24], electron beam evaporation^[25,26], and chemical vapor deposition^[27,28], have been reported to be used to fabricate VO₂ film. In order to control the stoichiometry of the film, high vacuum and high temperature which can lead high cost are needed. However, if VO₂ is to be used in application in real devices, the cost is very critical issue. For this reason, hydrothermal process and solution-based process are one of the best methods to produce the VO₂ nanodevices in view of various advantages; Easy and relatively cheap process.^[29] In this study, VO₂ (M) nanowires were synthesized by hydrothermal process. And various

nanodevices based on MIT of VO₂ nanowire were fabricated and characterized.

Figure 1-1 showed the flow chart of this thesis

Rest of the thesis is organized into the following chapters:

Chapter 2: Background knowledge pertinent to this dissertation is presented.

Chapter 3: Experimental techniques and characterization methods used to synthesis the VO₂ nanowires are introduced.

Chapter 4: The memristive properties of a single VO₂ nanowire with switching controlled by self- heating are presented.

Chapter 5: Effects of gas and pressure on memristive properties of a single VO₂ nanowire are presented.

Chapter 6: Thermochromic properties of VO₂ and polymer composite for smart window application are presented.

Chapter 7: A brief summary of the present work is provided. Scope for future work is discussed.

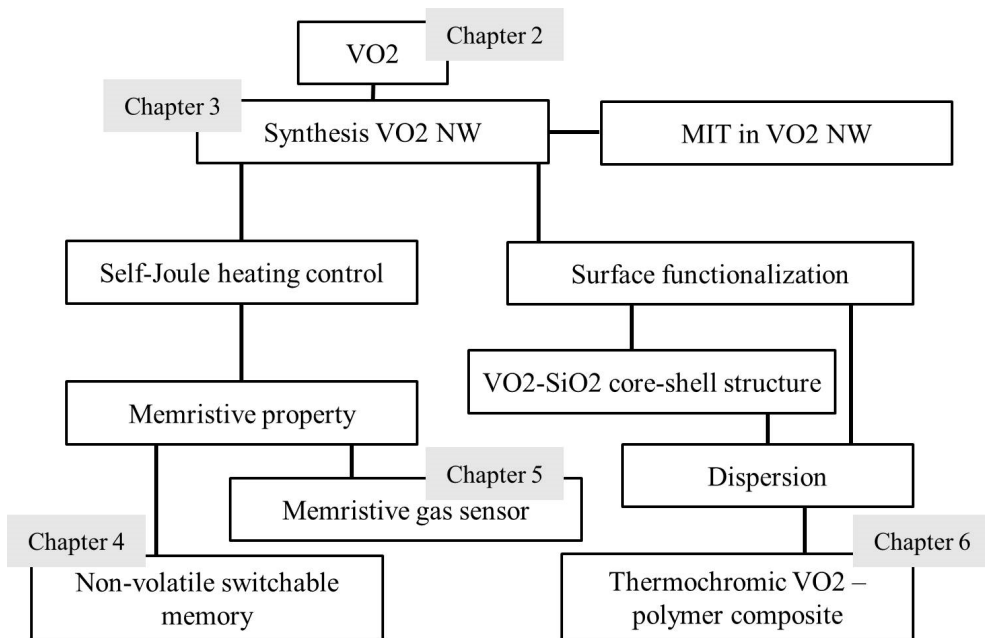


Figure 1-1 The flow chart of the rest chapter of this thesis

References

- [1] F.J. Morin, *Oxides which show a metal-to-insulator transition at the Neel temperature*, Phys. Rev. Lett. 3 (1959) 34
- [2] J.B. Goodenough, *The two components of the crystallographic transition in VO_2* , J. Solid. State. Chem. 3 (1971) 490
- [3] P. Jin and S. Tanemura, *Relationship between transition temperature and x in $V_{1-x}W_xO_2$ films deposited by dual-target magnetron sputtering*, Jpn. J. Appl. Phys. 34 (1995) 2459
- [4] C.N. Berglund and A. Jayaraman, *Hydrostatic-pressure dependence of electronic properties of VO_2 near semiconductor-metal transition temperature*, Phys. Rev. 185 (1969) 1034
- [5] A. Cavalleri, T. Dekorsy, H. H. W. Chong, J. C. Kieffer, R. W. Schoenlein, *Evidence for a structurally-driven insulator-to-metal transition in VO_2 : A view from the ultrafast timescale*, Phys. Rev. B 70 (2004) 161102
- [6] F. Chudnovskiy, S. Luryi, B. Spivak, *Future Trends in Microelectronics: The Nano Millennium*, In: S. Luryi, J. M. Xu, A. Zaslavsky (Eds), Wiley Interscience, New York (2002) 148–155
- [7] D. M. Newns, J. A. Misewich, C. C. Tsuei, A. Gupta, B. A. Scott, A. Schrott, *Mott transition field effect transistor*, Appl. Phys. Lett. 73 (1998) 780
- [8] H. Wang, X. Yi, S. Chen, X. Fu, *Fabrication of vanadium oxide micro-optical*

switches, Sens. Actuators A Phys. 122 (2005) 108

[9] M. J. Lee, Y. Park, D.S. Suh, E.H. Lee, S. Seo, D.C. Kim, R. Jung, B.S. Kang, S.E. Ahn, C.B. Lee, D.H. Seo, Y.K. Cha, I.K. Yoo, J.S. Kim, B.H. Park, *Two Series Oxide Resistors Applicable to High Speed and High Density Nonvolatile Memory*, Adv. Mater. 19 (2007) 3919

[10] R. A. Vaia, H. Ishii, and E. P. Giannelis, *Synthesis and Properties of Two-Dimensional Nanostructures by Direct Intercalation of Polymer Melts in Layered Silicates*, Chem. Mater. 5 (1993) 1694

[11] R. P. Andres, R. S. Averback, W. L. Brown, L. E. Brus, W. A. Goddard III, A. Kaldor, S. G. Louie, M. Moscovits, P. S. Peercy, S. J. Riley, R. W. Siegel, F. Spaepen and Y. Wang, *Research opportunities on clusters and cluster-assembled materials—A Department of Energy, Council on Materials Science Panel Report*, Mater. Res. 4 (1989) 704

[12] A. P. Alivisatos, *Semiconductor Clusters, Nanocrystals, and Quantum Dots*, Science 271 (1996) 933-937

[13] M. Wei , H. Sugihara , I. Honma , M. Ichihara , H. Zhou, *A New Metastable Phase of Crystallized $V_2O_4 \cdot 0.25H_2O$ Nanowires : Synthesis and Electrochemical Measurements*, Adv. Mater. 17 (2005) 2964

[14] C. Tsang, A. Manthiram, *Synthesis of Nanocrystalline VO_2 and Its Electrochemical Behavior in Lithium Batteries*, J. Electrochem. Soc. 144 (1999) 520

- [15] W. Li, J.R. Dahn, D.S. Wainwright, *Rechargeable Lithium Batteries with Aqueous Electrolytes*, Science 264 (1994) 1115
- [16] Y. Takahashi, M. Kanamori, H. Hashimoto, Y. Moritani, Y. Masuda, *Preparation of VO₂ films by organometallic chemical vapour deposition and dip-coating*, J. Mater. Sci. 24 (1989) 192
- [17] E.E. Chain, *Appl. Optical properties of vanadium dioxide and vanadium pentoxide thin films*, Opt. 30 (1991) 2782
- [18] I. Balberb, S. Trokman, *High-contrast optical storage in VO₂ films*, J. Appl. Phys. 46 (1977) 2111
- [19] I.P. Parkin and T.D. Manning, *Intelligent thermochromic windows*, Journal of Chemical Education 83 (2006) 393
- [20] H. Koo, H. W. You, K. E. Ko, O-J. Kwon, S-H. Chang, and C. Park, *Thermochromic Properties of VO₂ thin film on SiN_x buffered glass substrate*, Applied Surface Science, 277 (2013) 237
- [21] X.J. Wang et al., *Surface oxidation of vanadium dioxide films prepared by radio frequency magnetron sputtering*, Chinese Physics B 17 (2008) 3512
- [22] X.B. Wei, et al., *Growth mode and texture study in vanadium dioxide thin films deposited by magnetron sputtering*, Journal of Physics D: Applied Physics, 41 (2008) 055303
- [23] D.H. Kim and H.S. Kwok, *Pulsed laser deposition of VO₂ thin films*, Appl.

Phys. Lett. 65 (1994)

[24] M. Soltani, M. Chaker, E. Haddad, and R.V. Kruzelesky, *Thermochromic vanadium dioxide smart coatings grown on Kapton substrates by reactive pulsed laser deposition*, J. Vac. Sci. Technol. A24 (2006) 612

[25] G. Golan, A. Axelevitch, B. Sigalov, and B. Gorenstein, *Metal-insulator phase transition in vanadium oxides films*, Microelectron. J. 34 (2003) 255

[26] M. Fukuma, S. Zembutsu, and S. Miyazawa, *Preparation of VO₂ thin film and its direct optical bit recording characteristics*, Appl. Opt. 22 (1982) 265

[27] T. Maruyama and Y. Ikuta, *Vanadium dioxide thin films prepared by chemical vapour deposition from vanadium (III) acetylacetonate*, J. Mater. Sci. 28 (1993) 5073

[28] M.B. Sahana, G.N. Subbanna, and S.A. Shivashankar, *Phase transformation and semiconductor-metal transition in thin films of VO₂ deposited by low-pressure metalorganic chemical vapor deposition*, J. Appl. Phys. 92 (2002) 6495

[29] Y. Gao, C. Cao, L. Dai, H. Luo, M. Kanehira, Y. Ding and Z. L. Wang, *Phase and shape controlled VO₂ nanostructures by antimony doping*, Energy Environ. Sci. 5 (2012) 8708

Chapter 2. General background

2.1 Vanadium dioxide(VO₂)

Metal-to-insulator(MIT) transition in oxides is a topic of long-standing interest in condensed matter materials sciences. A number of reviews on MIT mechanisms and materials in the past 40 years indicate the consistent interest in this subject. Vanadium dioxide(VO₂) is well-known for its MIT transition at a certain critical temperature(T_c), as shown in Figure 2-1.^[1] The MIT of VO₂ is based on first-order phase transition. Above the transition temperature ($T_c = 67\text{ }^\circ\text{C}$), VO₂ is metallic and adopts the tetragonal rutile (P42/mmm) structure with chains of edge-shared VO₆ octahedral along the c-axis (the V–V distances along the chain are 2.880 Å). Below T_c , in the semiconducting monoclinic (P21/c) crystal structure, the vanadium atoms dimerized and have alternate V–V distances of 2.662 and 3.132 Å.^[1,2,3] The behavior causes large reversible changes of optical and magnetic properties, as well

as a change of resistivity by several orders of magnitude(Figure 2-2). Such property change made VO₂ to be considered as a material having high potentials for various applications, such as electronic switches, thermal sensors, and thermochromic smart windows.^[4,5,6,7,8,9,10,11,12,13]

VO₂ also shows an ultrafast ($\sim 10^2$ femtoseconds) transition when excited by a laser and exhibits metallic behavior under application of high electric-field ($\sim 10^6$ V/cm).^[14,15,16] This first-order MIT near room temperature has been widely studied over the last fifty years, yet the physics behind this intriguing phenomenon is not fully understood. The characteristics associated with MIT in VO₂ are fascinating scientifically, which let VO₂ have immense technological importance for potential applications in sensor- and memory-type applications.^[17]

The metal-to-insulator transition in VO₂ is characterized by abrupt orders of magnitude change in resistivity and increased reflectivity for infra-red light wavelengths (0.8-2.2 μm). Being a transition-metal oxide with narrow d-electron bands, MIT in VO₂ is extremely sensitive to small changes in extrinsic parameters such as pressure or doping.^[18,19,20] In bulk single crystals, the change in resistivity can be $\sim 10^3$ - 10^5 , with a hysteresis width of $\sim 1^\circ\text{C}$. On the other hand, hysteresis widths in thin films and in nanostructures are within the range of 3- 10°C and 30- 35°C , respectively.

Thin films and nanoparticles tend to better withstand the repeated thermal cycling,

and also the transition temperature can be lowered to room temperature by doping. Recent advances in thin film growth techniques and device fabrication methods have triggered numerous recommendations for technological applications of VO₂, such as, thermally activated optical switching and limiting^[21,22], thermal relays and energy management devices^[23,24], sensors and actuators^[25], micro-bolometers^[26,27], electrochromic and photochromic memory and optical devices^[28,29]. Two and three terminal devices utilizing the electric field induced switching of VO₂ is also an active area of research.^[30,31] A recent study^[32] has found that, materials synthesis, especially the VO₂/gate dielectric interface, plays an immensely important role in the response to the gate voltage, and thus controls the functioning of such electrically controlled devices.

Figure 2-3 shows the phase diagram for the vanadium-oxygen system.^[33] It can be seen that there are as many as 15 to 20 other stable vanadium oxide phases, such as, V₆O₉, V₆O₁₃, V₇O₁₃ and others that exhibit no semiconductor-to-metal transitions. The existence of these stable competing oxides presents a particular challenge to the growth of VO₂ in both bulk and thin film form. Therefore, to achieve optimum thermochromic properties, an elaborate synthesis procedure is required to ensure the formation of VO₂ and to avoid other undesirable vanadium oxide phases. Thin films of VO₂ have been deposited using several techniques, such as, reactive evaporation^[34,35], sputtering^[36,37], metal-organic chemical vapor deposition

(MOCVD)^[38,39], pulsed-laser deposition (PLD)^[40,41], and sol-gel deposition^[42,43].

But these techniques require the vacuum and high temperature process which can generate the high cost.

2.2 Vanadium dioxide nanodevice

In correlated oxides a frequently employed approach to induce MIT is thermal triggering, i.e., changing the temperature by heating or cooling. As shown in Figure 2-4 (part i), with a temperature increase from 341 to 344 K, the resistance of the VO₂ thin film decreases by nearly four orders. Other approaches to trigger the phase transition include electrical, optical, magnetic, and strain excitations.

Table 2-1 shows the principle and the application of VO₂. Not only heat (temperature) but also some other factor like stress, electric field, kindness or pressure of gas, photon can affect the phase transition properties such as transition temperature, transition voltage and resistivity.^[32,33] From the change of the transition properties of VO₂, sensor such as stress sensor, gas sensor, temperature sensor and optical sensor can measure or calculate a physical quantity. And some devices like oscillator, memristor and switch device can convert or save the electric signal by controlling the MIT properties.

2.3 Thermochromic Window based on VO₂

The world's available energy resources have been diminishing, and saving energy is one of the most effective ways to solve this energy shortage problem. It is estimated that buildings are responsible for more than 40% of energy use, primarily for space heating and cooling for indoor comfort. Smart window for energy saving are considered to be the first step for reducing heat transfer between the indoor and outside environments. Smart windows have already been developed, such as the Low-E window that possesses a low emissivity to achieve high thermal reflectivity of infrared light. Although the Low-E window has been widely used in the building industry, one of its disadvantages is that it cannot change its optical properties in response to temperature changes or different human needs. Based on the metal-to-insulator phase transition (MIT), vanadium dioxide (VO₂) smart windows can exhibit automatic change of the infrared transmittance in response to environmental temperatures without the use of any external energy, in comparison with other chromogenic windows, such as electrochromic or gasochromic, and it has recently attracted considerable attention. VO₂ undergoes a reversible MIT at ~68°C, that is accompanied by a structural phase transition from monoclinic (P21/c, M1 phase) to tetragonal (P42/mnm, R phase) symmetry with an abrupt change in optical properties from transmitting to highly reflecting particularly in the infrared spectral

region.

For a thermochromic smart window, the thermochromic material would be coated on the glass surface, and then it works due to the thermochromism of the coating layer. The change of optical properties with temperature is usually related to a structural phase change on passing through a critical temperature, T_c . At temperature below T_c , the material is relatively transparent in visible light and infrared range. This allows most of the solar radiation to pass through the window maximizing the heating effect of the sunlight and blockbody radiation within the building, keeping the interior warm. At temperatures above T_c , the thermochromic coating becomes infrared reflective, preventing thermal radiation from excessively heating the building interior while remaining visually transparent, enabling the optimum use of natural light.

2.4 Vanadium dioxide nanowire

Nanoscale materials often exhibit different physical and chemical properties compared with their bulk properties, and have attracted much attention because of their structural, electronic, and optical properties and their potential applications. One-dimensional (1D) nanostructure materials include nanotubes, nanorods, nanowires, nanofibers, nanobelts, and nanoribbons. The 1D structural VO₂ materials lead to a wide variety of potential applications including lithium batteries temperature-sensing devices, optical switching devices, and thermochromic smart window.

High quality single crystal VO₂ nanowire can show superior phase transition properties which can be represented as the sharp and abrupt change due to its crystalline perfectness. The various nanodevices which are based on polycrystalline VO₂ films were hampered by transition broadening and hysteresis effects due to strain or crystalline imperfectness. For these reasons, the single crystal VO₂ material with various nanostructures has been studied actively, due to the improved performance of the various nanodevices which are based on single crystalline VO₂.

Several methods have been reported to synthesize VO₂ nanowire. VO₂(B) nanobelts using ammonium metavanadate as a reagent was reported.^[44] VO₂(M) nanorods and nanowires were commonly synthesized at high temperature in an argon atmosphere using VO₂(M) powder as a starting material.^[45,46] Using

hydrothermal process, rutile VO_2 nanorods were obtained by the chemical reaction of KOH , V_2O_5 , and $\text{N}_2\text{H}_4 \cdot \text{H}_2\text{O}$. Needle-like $\text{VO}_2 \cdot \text{H}_2\text{O}$ was prepared using NH_4VO_3 and $\text{N}_2\text{H}_4 \cdot \text{H}_2\text{O}$ as reagents.^[47,48] For all of these systems, additional reagents were introduced into the reaction system. As such, the synthetic process is complicated, and might bring about an increase of impurity concentration in the final product.

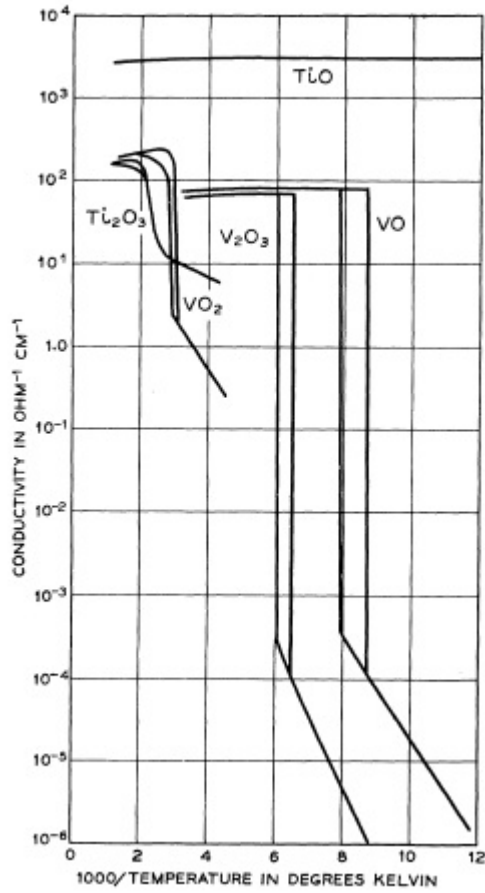


Figure 2-1 Conductivity as a function of reciprocal temperature for the lower oxides of titanium and vanadium.^[1]

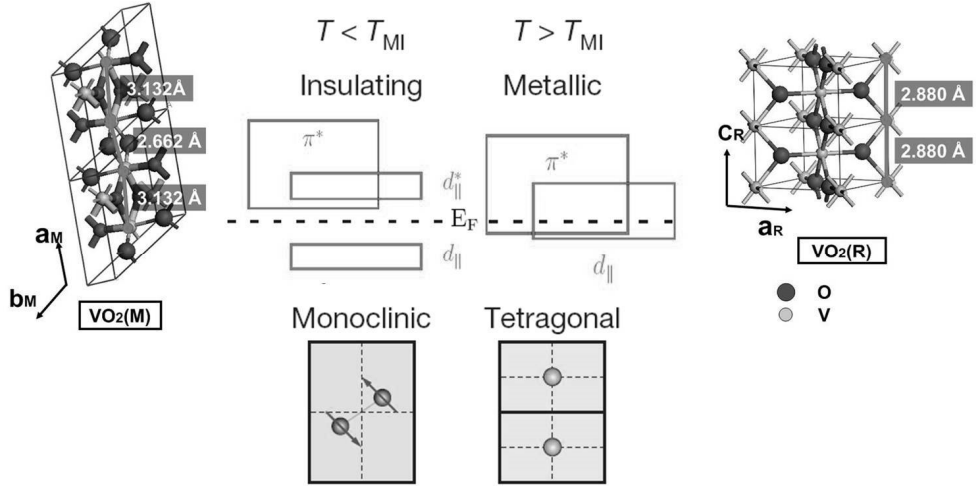


Figure 2-2. Schematic illustration of lattice of the two structural phases of VO_2 ^[2,3]

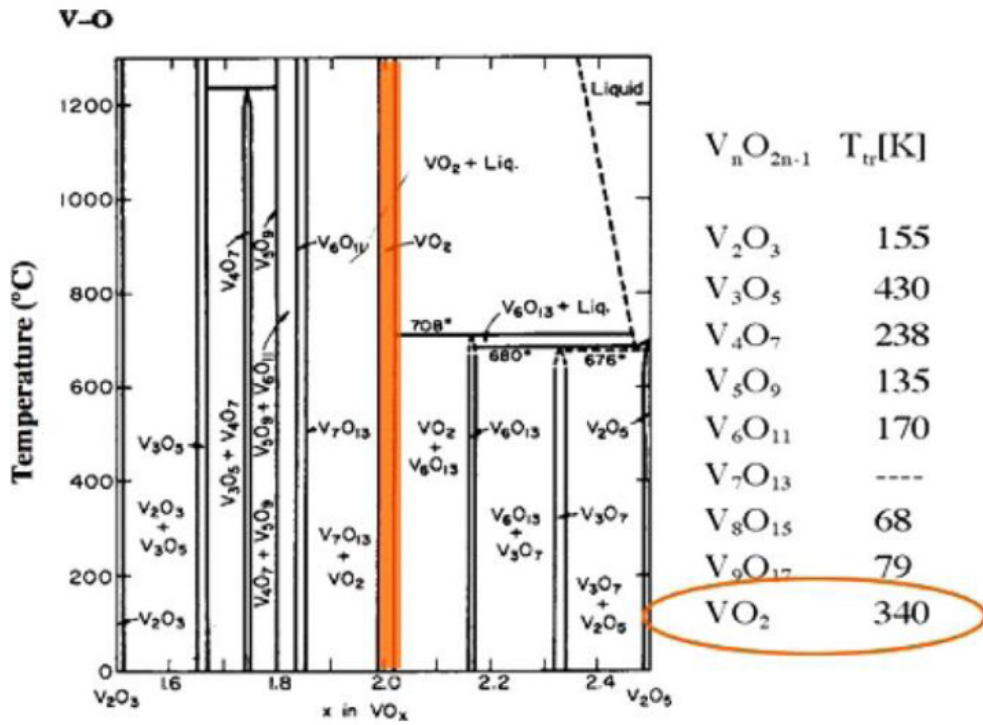


Figure 2-3. Phase diagram for the vanadium-oxygen system^[40]

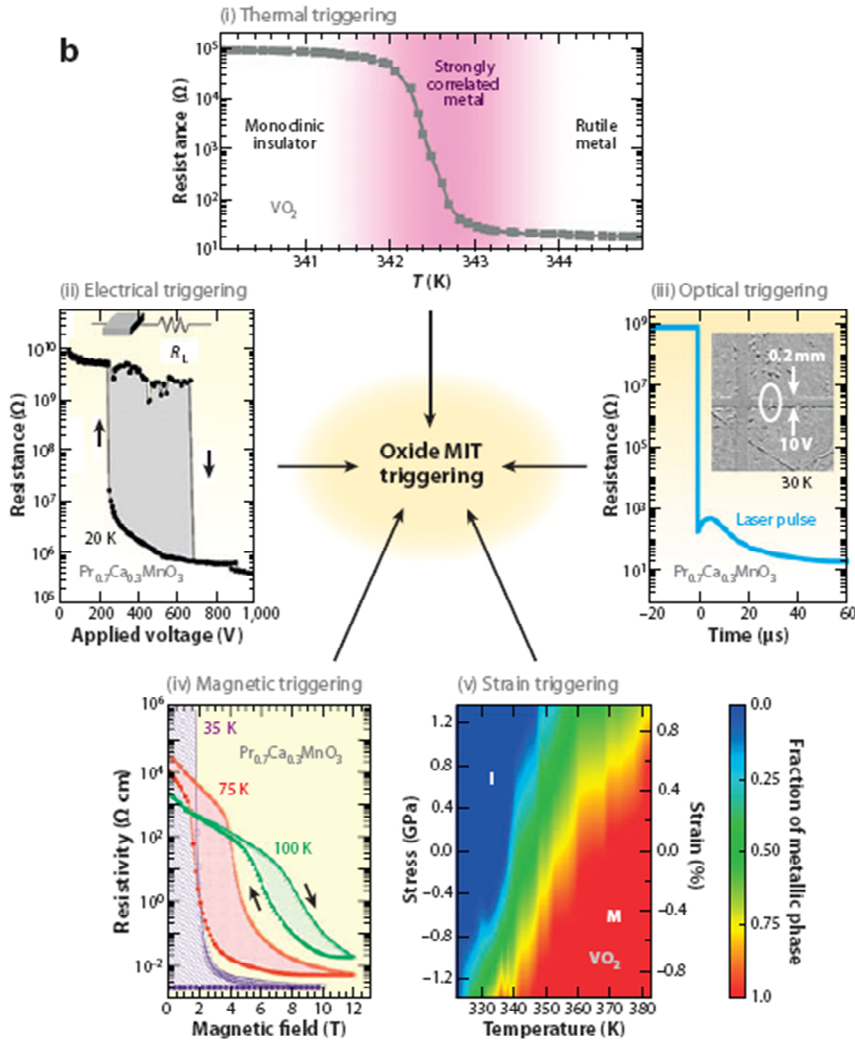


Figure 2-4. MIT-triggering approaches in correlated oxides. (i) Temperature-triggered MIT in VO_2 . (ii) Electrically triggered MIT in $\text{Pr}_{0.7}\text{Ca}_{0.3}\text{MnO}_3$. (iii) Optically triggered MIT in $\text{Pr}_{0.7}\text{Ca}_{0.3}\text{MnO}_3$. (iv) Magnetically triggered MIT in $\text{Pr}_{0.7}\text{Ca}_{0.3}\text{MnO}_3$. (v) Strain/stress effects on MIT in VO_2 .^[17]

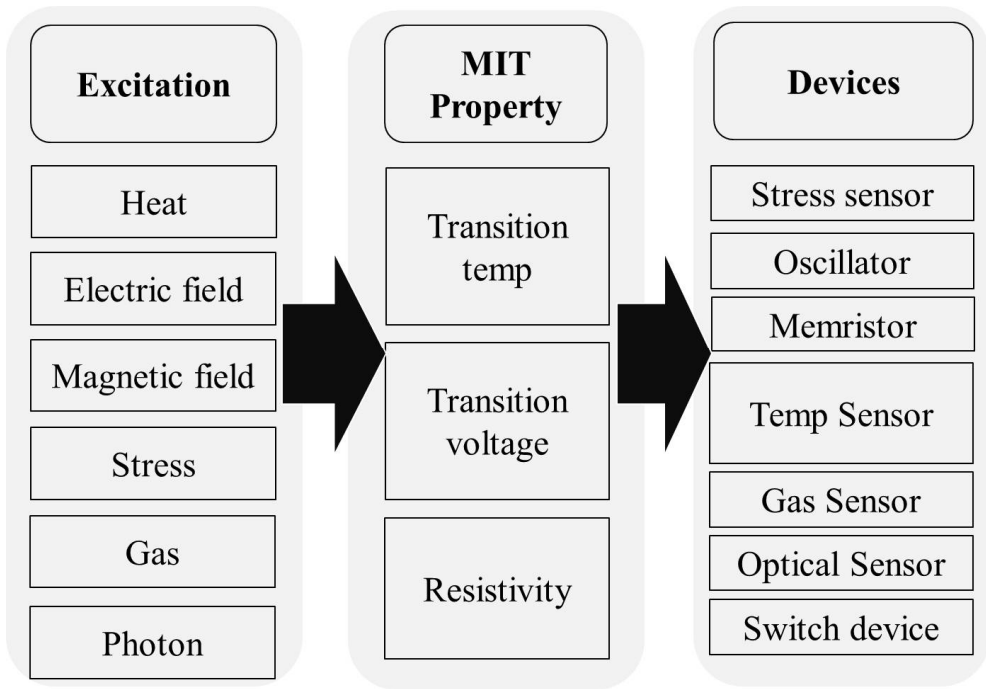


Table 2-1 VO₂ nano-devices

2.5 Reference

- [1] F.J. Morin, *Oxides which show a metal-to-insulator transition at the Neel temperature*, Phys. Rev. Lett. 3 (1959) 34
- [2] M. Nakano, K. Shibuya, D. Okuyama, T. Hatano, S. Ono, *Collective bulk carrier delocalization driven by electrostatic surface charge accumulation*, Nature, 487 (2012) 459
- [3] Y. Li, S. Ji, Y. Gao, H. Luo, M. Kanehira, *Core-shell VO₂@TiO₂ nanorods that combine thermochromic and photocatalytic properties for application as energy-saving smart coatings*, Scientific Reports, 3 (2013) 1370
- [4] D. Ruzmetov, G. Gopalakrishnan, J. D. Deng, V. Narayanamurti, S. Ramanathan, *Electrical triggering of metal-insulator transition in nanoscale vanadium oxide junctions*, J. Appl. Phys. 106 (2009) 083702
- [5] D. Ruzmetov, G. Gopalakrishnan, C. Ko, V. Narayanamurti, S. Ramanathan, *Three-terminal field effect devices utilizing thin film vanadium oxide as the channel layer*, J. Appl. Phys. 107 (2010) 114516
- [6] R. M. Briggs, I. M. Pryce, H. A. Atwater, *Compact silicon photonic waveguide modulator based on the vanadium dioxide metal-insulator phase transition*, Opt. Express, 18 (2010) 11192–201
- [7] Q. Gu, A. Falk, J. Q. Wu, O. Y. Lian, H. Park, *Current-driven phase oscillation and domain-wall propagation in W_xV_{1-x}O₂ nanobeams*, Nano Lett. 7

(2007) 363–66

[8] M. J. Dicken, K. Aydin, I. M. Pryce, L. A. Sweatlock, E. M. Boyd, *Frequency tunable near-infrared metamaterials based on VO₂ phase transition*, Opt. Express 17 (2009) 18330–39

[9] B. J. Kim, Y. W. Lee, B. G. Chae, S. J. Yun, S. Y. Oh et al. *Temperature dependence of the first-order metalinsulator transition in VO₂ and programmable critical temperature sensor*, Appl. Phys. Lett. 90 (2007) 023515

[10] E. Strelco, Y. Lilach, A. Kolmakov, *Gas sensor based on metal-insulator transition in VO₂ nanowire thermistor*, Nano Lett. 9 (2012) 2322–26

[11] F. Guinneton, L. Sauque, J.C. Valmalette, F. Cros, and J.R. Gavarrì, *Optimized infrared switching properties in thermochromic vanadium dioxide thin films: role of deposition process and microstructure*, Thin Solid Films 446 (2004) 287

[12] I. Takahashi et al., *Thermochromic V_{1-x}W_xO₂ thin films prepared by wet coating using polyvanadate solutions*, Jpn. J. of Appl. Phys. 35 (1996) 438

[13] K. Kato, et al., *Study on thermochromic VO₂ films grown on ZnO-coated glass substrates for “smart windows”*, Jpn. J. of Appl. Phys. Part 1- Regular Papers Short Notes Review Papers, 42 (2003) 6523

[14] P. Jin and S. Tanemura, *Relationship between transition temperature and x in V_{1-x}W_xO₂ films deposited by dual-target magnetron sputtering*, Jpn. J. Appl. Phys.

34 (1995) 2459

[15] C.N. Berglund and A. Jayaraman, *Hydrostatic-pressure dependence of electronic properties of VO₂ near semiconductor-metal transition temperature*, Phys. Rev. 185 (1969) 1034

[16] A. Cavalleri, T. Dekorsy, H. H. W. Chong, J. C. Kieffer, R. W. Schoenlein, *Evidence for a structurally-driven insulator-to-metal transition in VO₂: A view from the ultrafast timescale*, Phys. Rev. B 70 (2004) 161102

[17] Z. Yang, C. Ko, and S. Ramanathan, *Oxide Electronics Utilizing Ultrafast Metal-Insulator Transitions*, Annu. Rev. Mater. Res. 41 (2011) 337–67

[18] C.N. Berglund and H.J. Guggenheim, *Electronic properties of VO₂ near semiconductor-metal transition*, Phys. Rev. 1 (1969) 1022

[19] P. Jin and S. Tanemura, *Relationship between transition temperature and x in V_{1-x}W_xO₂ films deposited by dual-target magnetron sputtering*, Jpn. J. Appl. Phys. 34 (1995) 2459

[20] C.N. Berglund and A. Jayaraman, *Hydrostatic-pressure dependence of electronic properties of VO₂ near semiconductor-metal transition temperature*, Phys. Rev. 185 (1969) 1034

[21] M.F. Becker, A.B. Buckman, R.M. Walser, T. Lepine, P. Georges, and A. Brun, *Femtosecond laser excitation of the semiconductor-metal phase transition in VO₂*, Appl. Phys. Lett. 65 (1994) 1507

- [22] M. Soltani, M. Chaker, E. Haddad, R. Kruzelecky, and J. Margot, *Micro-optical switch device based on semiconductor-to-metallic phase transition characteristics of W-doped VO₂ smart coatings*, J. Vac. Sci. Technol. A25 (2007) 971
- [23] M. Soltani, M. Chaker, E. Haddad, and R.V. Kruzelesky, *Thermochromic vanadium dioxide smart coatings grown on Kapton substrates by reactive pulsed laser deposition*, J. Vac. Sci. Technol. A24 (2006) 612
- [24] T.D. Manning, I.P. Parkin, R.J.H. Clark, D. Sheel, M.E. Pemble, and D. Vernadou, *Intelligent window coatings: atmospheric pressure chemical vapour deposition of vanadium oxides*, J. Mater. Chem. 12 (2002) 2936
- [25] R.T. Rajendra Kumar, B. Karunagaran, D. Mangalaraj, S.K. Narayandass, P. Manoravi, M. Joseph, and V. Gopal, *Pulsed laser deposited vanadium oxide thin films for uncooled infrared detectors*, Sensors Actuators A107 (2003) 62
- [26] C. Chen, X. Yi, X. Zhao, and B. Xiong, *Characterizations of VO₂-based uncooled microbolometer linear array*, Sensors and Actuators A: Phy. 90 (2001) 212
- [27] C.D. Reintsema, E.N. Grossman, and J.N. Koch, *Improved VO₂ microbolometers for infrared imaging: operation on the semiconducting-metallic phase transition with negative electrothermal feedback*, Proc. SPIE 3698 (1999) 190-200, Infrared Technology and Applications XXV

- [28] G.V. Jorgenson and J.C. Lee, *Doped vanadium oxide for optical switching films*, Sol. Energy Mater. 14 (1986) 205
- [29] J.S. Chivian, M.W. Scott, W.E. Case, and N.J. Krasutsky, *An improved scan laser with a VO₂ programmable mirror*, IEEE J. Quantum Electron. 21 (1985) 383
- [30] C. Ko and S. Ramanathan, *Stability of electrical switching properties in vanadium dioxide thin films under multiple thermal cycles across the phase transition boundary*, J. Appl. Phys. 104 (2008) 086105
- [31] Z. Yang, C.H. Ko, V. Balakrishnan, G. Gopalakrishnan, and S. Ramanathan, *Dielectric and carrier transport properties of vanadium dioxide thin films across the phase transition utilizing gated capacitor devices*, Phys. Rev. B 82 (2010) 205101
- [32] D. Ruzmetov, G. Gopalakrishnan, C.H. Ko, V. Narayanamurti, and S. Ramanathan, *Three-terminal field effect devices utilizing thin film vanadium oxide as the channel layer*, J. Appl. Phys. 107 (2010) 114516
- [33] C.H. Griffith and H.K. Easwood, *Influence of stoichiometry on the metal-semiconductor transition in vanadium dioxide*, J. Appl. Phys. 45 (1974) 2201
- [34] G. Golan, A. Axelevitch, B. Sigalov, and B. Gorenstein, *Metal-insulator phase transition in vanadium oxides films*, Microelectron. J. 34 (2003) 255
- [35] M. Fukuma, S. Zembutsu, and S. Miyazawa, *Preparation of VO₂ thin film and its direct optical bit recording characteristics*, Appl. Opt. 22 (1982) 265

- [36] J.A. Thornton, *Plasma-assisted deposition processes: theory, mechanisms and applications*, Thin Solid Films 107 (1983) 3
- [37] F. Guinneton, L. Sauque, J.C. Valmalette, F. Cros, and J.R. Gavarri, *Optimized infrared switching properties in thermochromic vanadium dioxide thin films: role of deposition process and microstructure*, Thin Solid Films 446 (2004) 287
- [38] T. Maruyama and Y. Ikuta, *Vanadium dioxide thin films prepared by chemical vapour deposition from vanadium (III) acetylacetonate*, J. Mater. Sci. 28 (1993) 5073
- [39] M.B. Sahana, G.N. Subbanna, and S.A. Shivashankar, *Phase transformation and semiconductor-metal transition in thin films of VO₂ deposited by low-pressure metalorganic chemical vapor deposition*, J. Appl. Phys. 92 (2002) 6495
- [40] M. Borek, F. Qian, V. Nagabushnam, and R.K. Singh, *Pulsed laser deposition of oriented VO₂ thin films on R-cut sapphire substrates*, Appl. Phys. Lett. 63 (1993) 3288
- [41] A. Gupta, R. Aggarwal, P. Gupta, T. Dutta, R. J. Narayan, and J. Narayan, *Semiconductor to metal transition characteristics of VO₂ thin films grown epitaxially on Si (001)*, Appl. Phys. Lett. 95 (2009) 11915 (2009).
- [42] C. B. Greenberg, *Undoped and doped VO₂ films grown from VO(OC₃H₇)₃*, Thin Solid Films 110 (1983) 73

- [43] J. Livage, G. Guzman, F. Beteille, and P. Davidson, *Optical properties of sol-gel derived vanadium oxide films*, J. Sol–Gel Sci. Technol. 8 (1997) 857
- [44] J. F. Liu, Q. H. Li, T. H. Wang, D. P. Yu, Y. D. Li, *Metastable Vanadium Dioxide Nanobelt: Hydrothermal Synthesis, Electrical Transport, and Magnetic Properties*. Angew Chem. Int. Ed. 43(2004) 5048
- [45] B. S. Guiton, Q. Gu, A. L. Preto, M. S. Gudiksen, H. K. Park, *Temperature-controlled surface plasmon resonance in VO₂ nanorods*, J. Am. Chem. Soc. 2005, 127 (2005) 98.
- [46] Z. Gui, R. Fan, W. Q. Mo, X. H. Chen, L. Yang, S. Y. Zhang, Y. Hu, Z. Z. Wang, W. C. Fang, *Precursor Morphology Controlled Formation of Rutile VO₂ Nanorods and Their Self-Assembled Structure*, Chem. Mater. 14 (2002) 5053.
- [47] Z. Gui, R. Fan, X. H. Chen, Y. C. Wu, *A New Metastable Phase of Needle-like Nanocrystalline VO₂·H₂O and Phase Transformation*, J. Solid State Chem. 157 (2001) 250.

Chapter 3. Synthesis of VO₂ nanowire

3.1 Hydrate VO₂ nanowire synthesis

In order to apply VO₂ in various nanodevice application based on metal-to-insulator transition(MIT), the VO₂ nanowire would be a good candidate material due to its low dimension.^[1,2,3,4,5] Therefore, it is necessary to achieve pure VO₂ nanowire with excellent MIT properties by using low cost process. There were some reports about the synthesis of VO₂ nanowire; the vapor-liquid-solid method^[6], the thermal vapor transport method^[7,8,9], the hydrothermal reduction method^[10,11,12]. The vapor-liquid-solid method and the thermal vapor transport method are inefficiency process because these methods need the single crystal substrate, high temperature and vacuum pressure. The hydrothermal reduction method is also inefficiency method because some metastable phase of VO₂ which is produced in process.

Wei et al. reported the synthesis method of the hydrate VO₂ nanowire for application in battery.^[5] In this paper, hydrate VO₂ nanowire can be successively

synthesized from VO_2 powder which is starting materials, and any metastable phase is came out through the hydrothermal process. The producing principles is already reported as a hydrating–exfoliating–splitting model of $\text{V}_2\text{O}_4 \cdot 0.25\text{H}_2\text{O}$ nanowire formation from raw VO_2 particles. In a typical synthesis, 0.15 g of commercial VO_2 was dispersed into 15 mL of H_2O , and was then transferred into a 20 mL autoclave and kept in an oven at 150-230 °C for 1–7 days. The product was then filtered off and dried in air. Because VO_2 is a metastable phase, the $\text{V}_2\text{O}_4 \cdot 0.25\text{H}_2\text{O}$ with a layered structure is formed under hydrothermal conditions. The $\text{V}_2\text{O}_4 \cdot 0.25\text{H}_2\text{O}$ has the nanosheets crystal structure. In order to release the strong stress and lower the total energy, the nanosheets are split, which results in the formation of nanowires..

The morphology and size of the resulting product after hydrothermal and annealing process are shown in Figure 3-1. Figure 3-1 contains the schematic of the hydrating–exfoliating–splitting model^[5] and the field emission scanning electron microscope(FESEM) images to inform the change of the nanostructure and morphology with increasing reaction time. In first, VO_2 powder is hydrated and its morphology change to layered structure (Figure 3-1 (a)). As reaction time increasing, the layered structure hydrated VO_2 powder is expolating and splitting to the nanosheet and the nanowire (Figure 3-1 (b)). After 3 days in hydrothermal process, all VO_2 powder change to the nanowire and the diameter of nanowire is

getting uniform (Figure 3-1 (c)). The hydrothermal process was performed for various times from 8 hours to 7 days at 220 °C. As the process time increased, the splitting and hydration of VO₂ hydrate nanowire more occurred and the nanowire became thinner. But after 7 days, the limit of a convergent of the diameter was about 60nm. This is because the thinner nanowire than the nanowire with the diameter about 60nm could have higher the total energy due to the large surface-to-volume fraction.

Figure 3-2 show FESEM images of nanowires which were carried out hydrothermal process for various temperature from 180 to 220 °C. As the process temperature increased, the nanowire became thinner. The higher temperature provided the abundant heat energy which could make more frequent hydration and splitting. But the polyurethane bottle couldn't sustain at higher temperature over 220 °C.

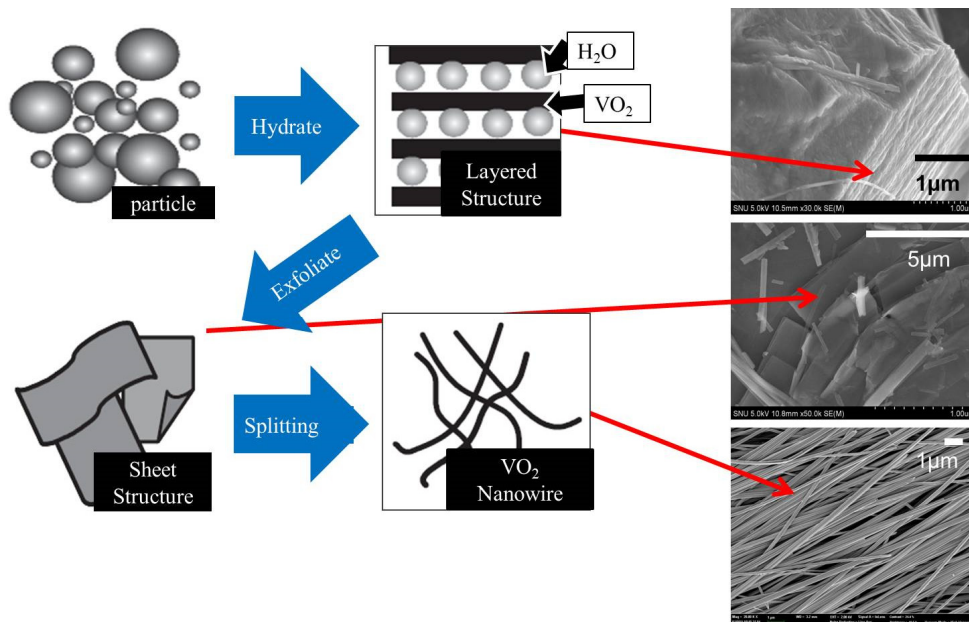


Figure 3-1 Schematic of the hydrating–exfoliating–splitting model and FESEM images

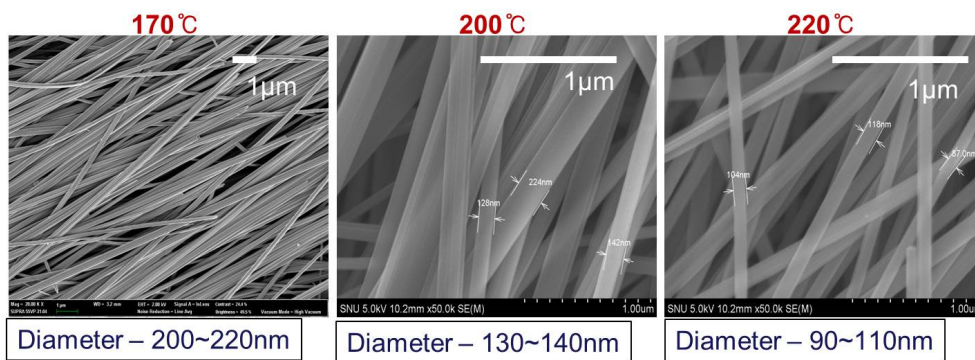


Figure 3-2 FESEM images of nanowires which were carried out hydrothermal process for various temperature from 180 to 220 °C for 3 days

3.2 Dehydrating process : post annealing

In order to investigate the properties of the single VO₂ nanowire, hydrate VO₂ nanowire should be dehydrated by post annealing process. Figure 3-3 showed the XRD and TGA results. In XRD result which is colored black, the peak from hydrate phase was observed ($2\theta \approx 10$ degree). In TGA result which is colored black, the weight of VO₂ hydrate decreased over 100°C in N₂ atmosphere. Especially over 300°C, the weight of hydrate nanowire decreased rapidly. This mass reduction came from the dehydrating of VO₂ hydrate. The annealing process for 4 hours at 400 °C in N₂ atmosphere is very optimized condition for dehydrating of VO₂ hydrate. The results which were colored red in Figure 3-3 were XRD and TGA result of VO₂ nanowire after annealing process. The peak from hydrate phase ($2\theta \approx 10$ degree) was not observed, and the peaks were corresponded to the VO₂(M) phase[JCPDS 44-0252]. No peaks of any other phases or impurities were observed, suggesting the conversion to pure VO₂(M) nanowire is complete. In TGA result, no mass reduction observed over 400°C. In conclusion, pure VO₂(M) nanowire without any hydrate phase were obtained by hydrothermal process which was followed by annealing.

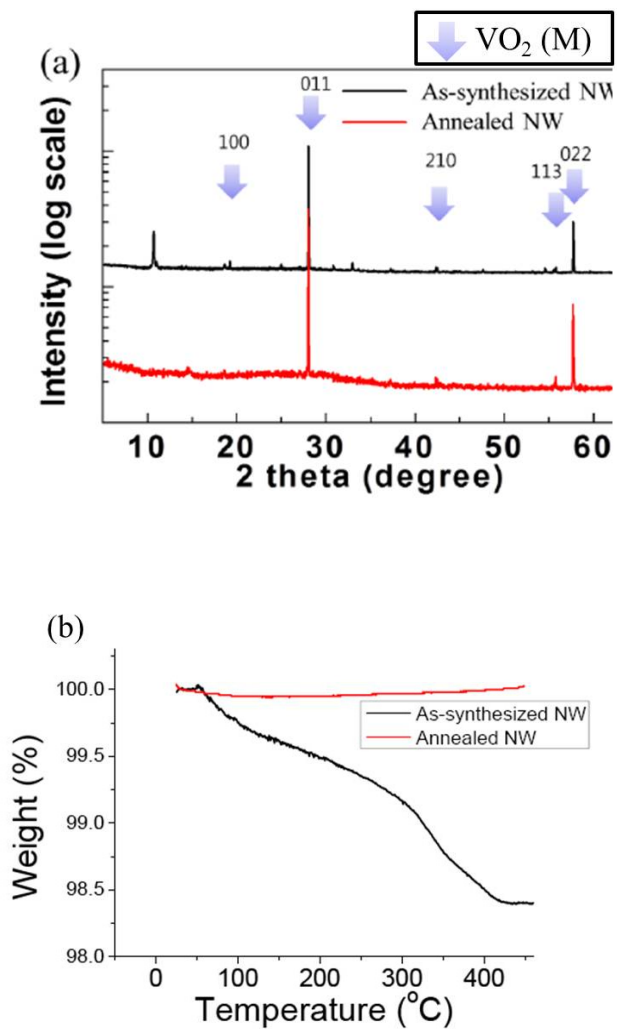


Figure 3-3 XRD (a) and TGA (b) result of VO₂ hydrate nanowire and VO₂ nanowire after annealing process

3.3 Metal-to-insulating transition properties of VO₂ nanowire

In order to investigate MIT properties of annealed VO₂ nanowires, the differential scanning calorimetry (DSC) analysis (Figure 3-4) and TGA analysis were carried out. During the heating and cooling cycles, the endothermic and exothermic peaks are observed at ~68°C and ~59°C, respectively in DSC analysis. But there was no mass change at ~68°C and ~59°C in TGA analysis. This result showed that the endothermic and exothermic peaks were came from the phase transitions from M → R and R → M. The observed transition temperature was same as reported values of VO₂ bulk.^[13] The hysteresis clearly shows that the VO₂ nanowires can exhibit the characteristic of the phase transition like the VO₂ bulk.

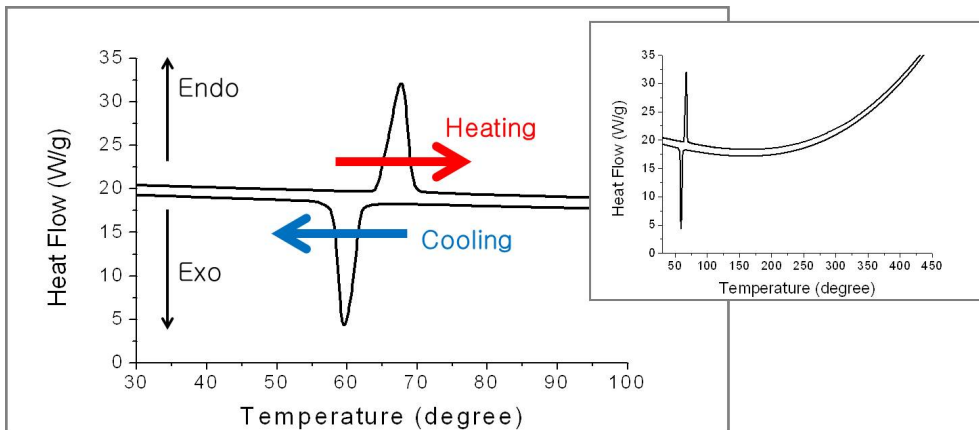


Figure 3-4 Differential scanning calorimetry (DSC) results of annealed VO₂ nanowires

3.4 Reference

- [1] J. F. Liu, Q. H. Li, T. H. Wang, D. P. Yu, Y. D. Li, *Metastable Vanadium Dioxide Nanobelt: Hydrothermal Synthesis, Electrical Transport, and Magnetic Properties*. *Angew Chem. Int. Ed.* 43(2004) 5048
- [2] B. S. Guiton, Q. Gu, A. L. Preto, M. S. Gudiksen, H. K. Park, *Temperature-controlled surface plasmon resonance in VO₂ nanorods*, *J. Am. Chem. Soc.* 2005, 127 (2005) 98.
- [3] Z. Gui, R. Fan, W. Q. Mo, X. H. Chen, L. Yang, S. Y. Zhang, Y. Hu, Z. Z. Wang, W. C. Fang, *Precursor Morphology Controlled Formation of Rutile VO₂ Nanorods and Their Self-Assembled Structure*, *Chem. Mater.* 14 (2002) 5053.
- [4] Z. Gui, R. Fan, X. H. Chen, Y. C. Wu, *A New Metastable Phase of Needle-like Nanocrystalline VO₂·H₂O and Phase Transformation*, *J. Solid State Chem.* 157 (2001) 250.
- [5] M. Wei, H. Sugihara, I. Honma, M. Ichihara, and H. Zhou, *A New Metastable Phase of Crystallized V₂O₅·0.25H₂O Nanowires: Synthesis and Electrochemical Measurements*, *Adv. Mater.* 17 (2007) 296
- [6] J. Maeng, T. Kim, G. Jo, T. Lee, *Fabrication, structural and electrical characterization of VO₂ nanowires*, *Materials Research Bulletin* 43 (2008) 1649–1656
- [7] J. M. Baik, M. H. Kim, C. Larson, A. M. Wodtke, M. J. Moskovits,

Nanostructure-Dependent Metal–Insulator Transitions in Vanadium-Oxide Nanowires, J. Phys. Chem. C. 112 (2008), 13328–13331

[8] J. M. Baik, M. H. Kim, C. Larson, C. T. Yavuz, G. D. Stucky, A. M. Wodtke, and M. Moskovits, *Pd-Sensitized Single Vanadium Oxide Nanowires: Highly Responsive Hydrogen Sensing Based on the Metal-Insulator Transition*, Nano Lett. 9 (2009) 3980

[9] E. Strelco, Y. Lilach, A. Kolmakov, *Gas sensor based on metal-insulator transition in VO₂ nanowire thermistor*, Nano Lett. 9 (2012) 2322

[10] J. Shidong, Z. Yangang, Z. Feng, J. Ping, *Direct formation of single crystal VO₂(R) nanorods by one-step hydrothermal treatment*, Journal of Crystal Growth 312 (2010) 282

[11] J. Shidong, Z. Yangang, Z. Feng, J. Ping, *Synthesis and phase transition behavior of w-doped VO₂(A) nanorods*, Journal of the Ceramic Society of Japan, 118 (2010) 867

[12] J. Shidong, Z. Yangang, J. Ping, *Phase transition of single crystal VO₂(R) nanorods in solution revealed by reversible change in surface charge state and structure*, Materials Letters, 65 (2011) 708

[13] F.J. Morin, *Oxides which show a metal-to-insulator transition at the Neel temperature*, Phys. Rev. Lett. 3 (1959) 34

Chapter 4. The memristive properties of a single VO₂ nanowire with switching controlled by self-heating

4.1 Introduction

Development of low-power and high-density memory device has attracted considerable interest with integrated circuit technology because of the physical limits of scalability in traditional memory device like DRAM. Rationally designed materials and technologies have been the subjects of active research for the next generation of universal memories. The memory device should exhibit not only high capacity and low-power consumption but also high-speed operation and long retention based on simple structures.^[1] Recently, a memristor capable of behaving as the two-terminal non-volatile and switchable resistive memory was demonstrated, which is well known as the fourth fundamental circuit element theoretically predicted by L. Chua in 1971.^[2] Since the memristor can achieve both high integration density and low switching power consumption due to the high scalability down to only a few nanometers, it has been one of the most attractive devices for the next-generation memory technology.^[3] Various materials with

switchable and retainable resistance have been used to realize the memristor memory, which include protein,^[4,5] TiO₂,^[6] polyaniline,^[7] Si,^[8] MgO,^[9,10] and vanadium dioxide (VO₂).^[11,12,13,14] VO₂ is one of the most notable materials due to fast response time and large range of accessible resistance values through a metal-to-insulator transition (MIT). The MIT, which is based on the structural phase transition between metallic tetragonal-rutile (VO₂(R)) and insulating monoclinic structure (VO₂(M)), can lead to change in electrical resistance of about four orders of magnitude and pinched hysteresis loops in I-V curve.^[15,16,17,18,19] The temperature at which this MIT occurs can be changed by doping, lattice mismatch, external strain and controlling grain size.^[20,21,22,23,24,25,26] Over the years, memristors based on thin-film VO₂ have been demonstrated as the memory device with switchable and retainable resistances. The change of resistance was obtained by providing pulse-type energy sources such as voltage, light, and current, which played the role of trigger for the MIT.^[12,13,14] The resistance could be retained by keeping the temperature near the transition temperature (T_c) of about 68°C using an additional heating source. However, although the switched resistance can be maintained well near the T_c, it can only provide small range of accessible resistance of less than two orders of magnitude at fixed temperature because only a part of the hysteresis is used. ^[12,13,14] Furthermore, using additional heating source for maintaining the resistance can make it difficult to achieve low power consumption and high density

integration. Thus, it is necessary to develop innovative strategy toward achieving low-power, high-density and two-terminal memristor for practical application in non-volatile memory device. In this chapter, we investigated the memristive behavior of the single VO₂ nanowire by observing the changeable and retainable resistances which can be controlled by pulses and low bias voltage. This is a key step towards the development of new low-power and two-terminal memory devices for next-generation non-volatile memories.

4.2 Experiment procedure

In this work, we report, for the first time, a two-terminal memristor memory based on a single VO₂ nanowire which can not only provide switchable resistances in a large range of about four orders of magnitude but also maintain the resistances by a low bias voltage. The VO₂ nanowires were synthesized by hydrothermal method,^[27] followed by thermal annealing process to form monoclinic VO₂ phase. In order to investigate the electrical properties and memristive properties of a single VO₂ nanowire, the nanowire was connected to the silver electrodes by using silver paste. The memristive behavior of the single VO₂ nanowire was confirmed by observing the switching and non-volatile properties of resistances when voltage pulses and low bias voltage were applied, respectively. Furthermore, multiple retainable resistances in a large range of about four orders of magnitude can be utilized by controlling the number and the amount of voltage pulses under the low bias voltage. For the low-power, high-density, and non-volatile memristor memory, it is important to make it a two-terminal device without using any additional heating source. Thus, we focused our research on designing single VO₂ nanowire-based memristor with pinched hysteresis loop through self-Joule heating generated by a low bias voltage.

4.3 Results and discussion

Figure 4-1(a) showed field emission scanning electron microscopy (FE-SEM) images of the nanowires and silver contact. A single nanowire with length and thickness of $\approx 30\mu\text{m}$ and $\approx 160\text{ nm}$, respectively, was connected to the silver electrodes. The VO_2 nanowire was synthesized by hydrothermal process for 3 days at $220\text{ }^\circ\text{C}$, followed by annealing for 4 hours at $400\text{ }^\circ\text{C}$ in N_2 atmosphere. After 3 days of hydrothermal process, all the VO_2 powder was changed into the nanowires with 80 to 160 nm diameters. In order to investigate the potential of the device for a heat-source-free memristor based on a single VO_2 nanowire, voltage-resistance curves of the single VO_2 nanowire were measured at room temperature and $100\text{ }^\circ\text{C}$, and the results are shown in Figure 4-1(b). While the resistance of the as-synthesized nanowire without the annealing process was not changed with the bias voltage at room temperature, that of the annealed VO_2 nanowire was reduced by ~ 4 orders of magnitude upon $\text{M}\rightarrow\text{R}$ transition.^[28,29] It is probably due to the presence of hydrate phases in the as-synthesized nanowires that cannot drive the MIT. On the other hand, since the annealed nanowire is $\text{VO}_2(\text{M})$ without any hydrate phases, the MIT can be driven by the bias voltage, which can generate self-Joule heating. The resistance value of the annealed nanowire after the MIT with the bias voltage over $\sim 0.34\text{V}$ at room temperature was similar to that obtained at 100°C . This means that the MIT of the single VO_2 nanowire can be driven by the bias voltage as

well as the direct heating. Furthermore, since the MIT of the single VO₂ nanowire took place with the low bias voltage of about 0.34 V in V-R curve due to its extremely small volume, which is much lower than those previously reported, devices based on a single VO₂ nanowire can have the advantage of low-power consumption.^[30,31,32]

Figure 4-2 shows the schematic of the single VO₂ nanowire-based memristor of which the two ends were electrically connected to copper wires with silver paste. The MIT was induced by the Joule heating, and the hysteresis behavior was observed (the transition voltage for the M to R transition was larger than that for the R to M transition). This hysteresis behavior leads to the non-linear I-V characteristic and eventually enables the switched resistance to be maintained. It was reported that the switchable resistance can be obtained by realizing the mixed state of metallic and insulating phases in the VO₂.^[12,13,14] If energy, such as heat or light, is large enough to drive MIT is applied to VO₂, all of the insulating phase (I in Figure 4-2) can be transformed into metallic phase (IV). But when the applied energy is not large enough for the complete phase transition, the metallic phase can be partially formed in the insulating phase (II and III) owing to the percolative nature of the MIT in VO₂.^[14,33,34] In other words, the mixed states of metallic and insulating phase can be obtained during the MIT of a single VO₂ nanowire, and the relative amount of each phase (metallic/insulating phase ratio) of the mixed state

can be controlled by the amount of applied energy, which can lead to various resistance values.

In order to realize low power consumption, the memsitive system which can be controlled by self-Joule heating was designed. In the memsitive system which can be controlled by self-Joule heating, two kinds of voltage sources should be were supplied; one is the bias voltage for measuring resistance, and the other is the voltage pulse for triggering MIT in the VO₂ nanowire. Figure 2-3 shows the schematic of these two kinds of voltage and explanations of role. The bias voltage for reading the resistance could also perform to generate the Joule-heating which can replace of additional heating stage. The voltage pulse could trigger the partial MIT in VO₂ nanowire.

Prior to demonstrating the retainable and switchable characteristic of a single VO₂ nanowire, it is needed to determine the amount of bias voltage which can maintain the switched resistance through self-Joule heating. In previous results,^[12,13,14] the specific temperature, which can maintain the switched resistance, was determined between the two transition temperatures in heating and cooling cycle of the hysteresis in R-T curve because the resistance can be changed only in the hysteresis loop^[12,13,14]. Likewise, since the temperature of the nanowire can be controlled by self-Joule heating through the application of specific bias voltage^[35],

in order to find out the amount of the specific bias voltage, we investigated the resistance change of the nanowire when different amounts of bias voltages were applied inside the hysteresis loop (Figure 2-2). When the bias voltage was over 0.3 V, the MIT took place over time because the temperature of the nanowire was increased over $M \rightarrow R$ transition temperature by Joule heating. When the bias voltage was below 0.3 V, the mixed state returned to the initial state (i.e. insulating state) over time because the nanowire was cooled below the $R \rightarrow M$ transition temperature. On the other hand, when the bias voltage of 0.3 V was applied in the nanowire, the $M \rightarrow R$ transition (I, II, III, and IV in Figure 4-2) did not occur by the self-Joule heating, and the resistance of the mixed state did not return to that of the initial state through $R \rightarrow M$ transition (II, III, IV \rightarrow I). Using this specific bias voltage of 0.3 V, the retainable and switchable characteristics were realized by applying various voltage pulses for 0.25 second under the bias voltage. As shown in Figure 4-4, the resistance rapidly dropped to lower values depending on the amount of the voltage pulse, and then they were maintained for over 5 minutes. In other words, when the 0.3 V bias voltage is applied at room temperature, the nanowire can be in the thermally stable state; in which the amount of the heat absorption in the nanowire by the self-Joule heating would be almost the same as that of heat desorption into the surrounding ambient. In the thermally stable state, the nanowire does not undergo $M \rightarrow R$ transition from insulating state or $R \rightarrow M$

transition from mixed state. Of course, the amount of the specific bias voltage, which can retain the switched resistance, may change depending on the dimension of nanowires and the ambient temperature, but this result clearly shows that the retainable and switchable characteristics in a single VO₂ nanowire can be realized by the application of voltages without using any additional heating source.

For practical device application, well-defined controllability of resistance based on the retainable and switchable characteristics is one of the most important requirements. For switching device application of VO₂, the MIT induced by external strain have been reported.^[25,26] Under the same applied voltage, the low resistance status of VO₂ single domain can be switched to a high resistance status by stretching the substrate. The VO₂ device of these previous works shows only two resistance states, however, the resistance of memristor can be changed into various values by voltage pulse. The change of resistance was measured with the amount (1, 3, 5, and 10 V) and the number (up to 10 times) of voltage pulses of a single VO₂ nanowire, as shown in Figure 4-5. Before applying the voltage pulses, the VO₂ nanowire was in the insulating state which has a resistance of $\sim 10^{11}\Omega$. When the voltage pulse was applied to the single nanowire, the resistance dropped to lower value due to the partial formation of the metallic phase in the insulating phase. This resistance drop can be obtained by low voltage pulse of 1 V, and as the amount of voltage pulse increases to 3, 5, and 10V, the resistance can be decreased

to values which are much lower than that of insulating state. And also, the resistance decreases in a step-by-step mode corresponding to the application of repeated voltage pulses. The change of resistance is largest when the first voltage pulse is applied and decreases as more pulses are applied, and the resistance is saturated to the value of $\sim 10^7 \Omega$, which is the same as that of the metallic phase (IV in Figure 4-2). As shown in the insets of Figure 4-5, the resistance shows switching property with changes of less than one order of magnitude near $\sim 10^7 \Omega$. These results suggest that the amount of change in resistance can be controlled even within less than one order of magnitude by the amount and the number of voltage pulses. The total range of accessible resistance is approximately 4 orders of magnitude which is similar to the change of resistance in MIT (that between I and IV in Figure 4-2) of a single nanowire. In previous reports,^[12,13,14] the resistance was controlled by heating stage, and the ranges of accessible resistance at fixed temperature was less than two orders of magnitude because they could use only a part of the hysteresis loop. However, when self-Joule heating is used instead of the direct heating with additional heat source, the nanowire can have a range of temperature, and any resistance value in-between those of metallic and insulating states can be accessed.

The single VO₂ nanowire can be utilized in an information storage device due to its switchable and retainable resistance that can be easily controlled by applying

voltage. In order to investigate the applicability of the single VO₂ nanowire in the information storage device, we measured the change of resistance which is the results of the voltage pulse for writing and the zero voltage for erasing/resetting. The changes of the resistance of a single VO₂ nanowire when two different voltage pulses are applied repeatedly are shown in Figure 4-6. The initial state (at room temperature without voltage pulse) of the VO₂ single nanowire is insulating state ($\sim 10^{11}\Omega$), and two different values of resistance are obtained by applying voltage pulse of 3 and 5V for 0.25 second under the bias voltage of 0.3 V. The 3V and 5V voltage pulses decrease the resistance by over 1 and 2 orders of magnitude, respectively. And the resistances can be retained for over 25 seconds by bias voltage. Considering the resistance change with less than 1 order of magnitude in the previous report,^[12,13,14] this large change of resistance can help obtain reliable switching performance in the information storage application. As it is already explained in Figure 3, the change of resistance is largest when the first voltage pulse is applied, and as the state is approaching to the metallic state, larger energy is required to achieve new lower resistance states. Therefore, the reliable switching property with large resistance change by low voltage pulse can be successfully achieved by setting the state of VO₂ nanowire near the insulating state. The voltage pulse under bias voltage, however, can drive only one-way transformation (M \rightarrow R transition). In order to reset VO₂ into the initial state, different operations like zero

bias voltage is needed. Applying zero voltage bias to the VO₂ nanowire for 2 seconds can reset nanowire to the initial state. After resetting, the resistances can be switched reproducibly by applying voltage pulse under the bias voltage. This shows that the VO₂ nanowire, when the change of resistance is controlled by the self-Joule heating, has the advantage of having access to wide range of resistances and obtaining reliable resistance switch, which can lead to high-performance non-volatile memory switch device with improved stability and operating speed.

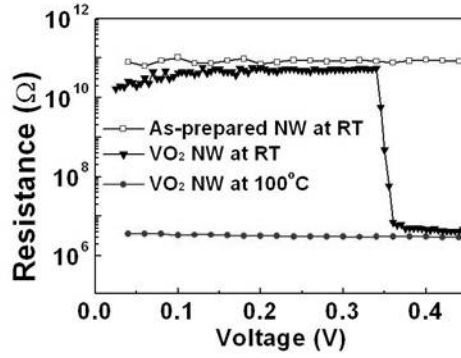
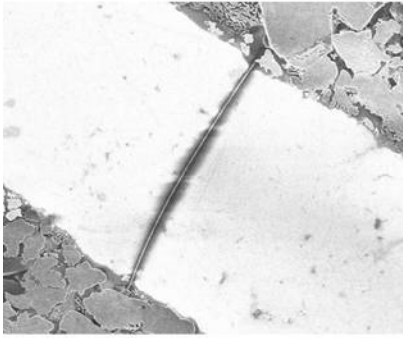


Figure 4-1 FESEM image of a single VO₂ nanowire and silver contact. Resistance with bias voltage of annealed VO₂ nanowires at room temperature (triangle), at 100 °C (circle), and an as-synthesized nanowire at room temperature (square).

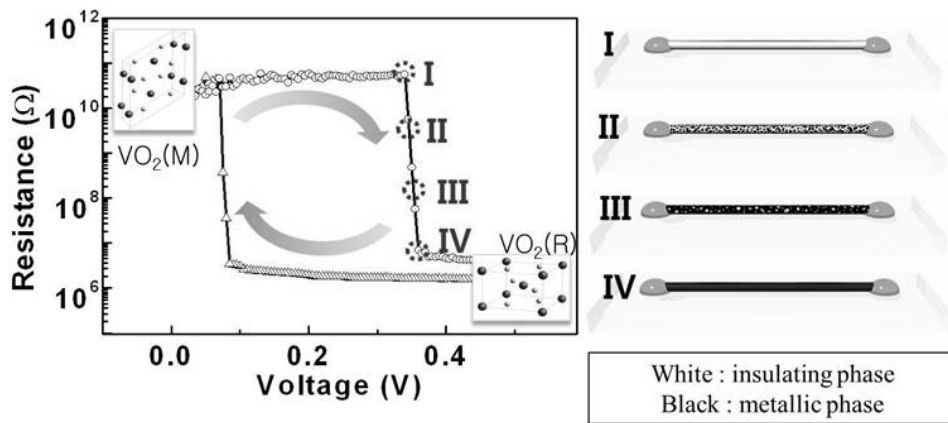


Figure 4-2 The resistance–voltage (R–V) hysteresis curve. Insets show the crystal structures of VO₂ (M) and VO₂ (R). Schematics showing the gradual change of phases inside the nanowire at different points marked in the R–V curve. Black and white parts denote the metallic and insulating phase of nanowire, respectively, and the mixed state shows the presence of multiple resistance of VO₂ nanowire.

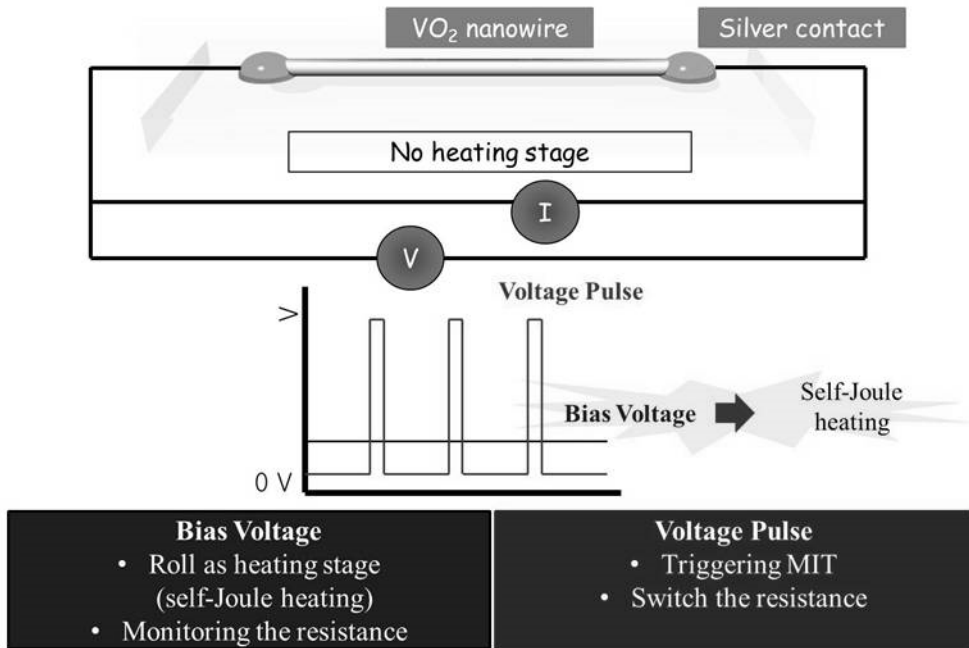


Figure 4-3 Schematic of these two kinds of voltage and explanations about the roles of each voltage; the bias voltage used for monitoring the resistance could be a roll as heating stage, the voltage pulse could trigger the MIT and switch the resistance.

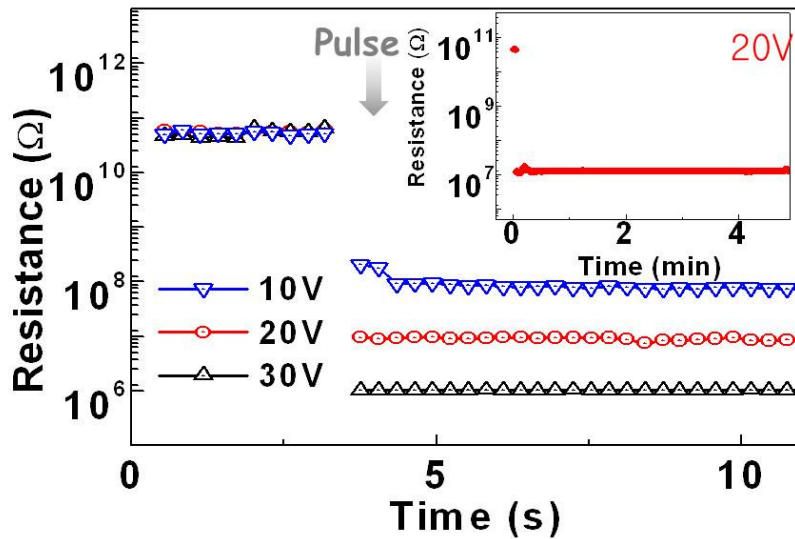


Figure 4-4 Resistance of annealed VO₂ nanowires at room temperature with 0.3 V voltage bias. The 30 V (diamond), 20 V (triangle), and 10 V voltage pulses (circle) are applied for 0.25 seconds. Inset graph shows the change of resistance for 5 minutes with 0.3 V voltage bias and 20 V voltage pulse

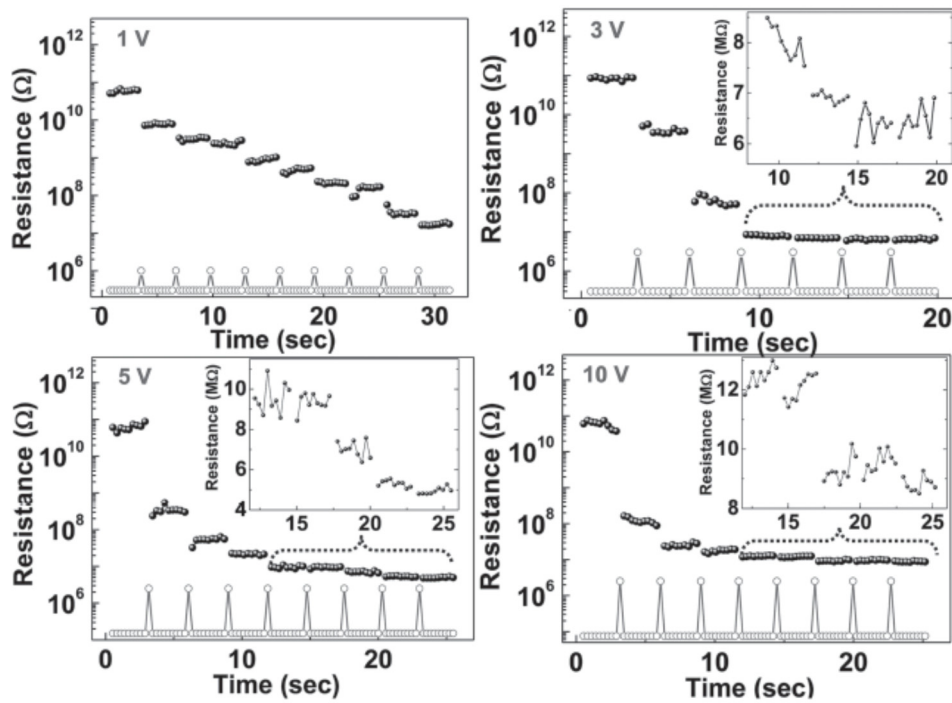


Figure 4-5 The change of resistance measured with the amount (1, 3, 5, and 10 V) and the number (up to 10 times) of voltage pulses of a single VO₂ nanowire. The well-defined multiple resistance values with large range can be obtained by controlling the amount and the number of voltage pulse.

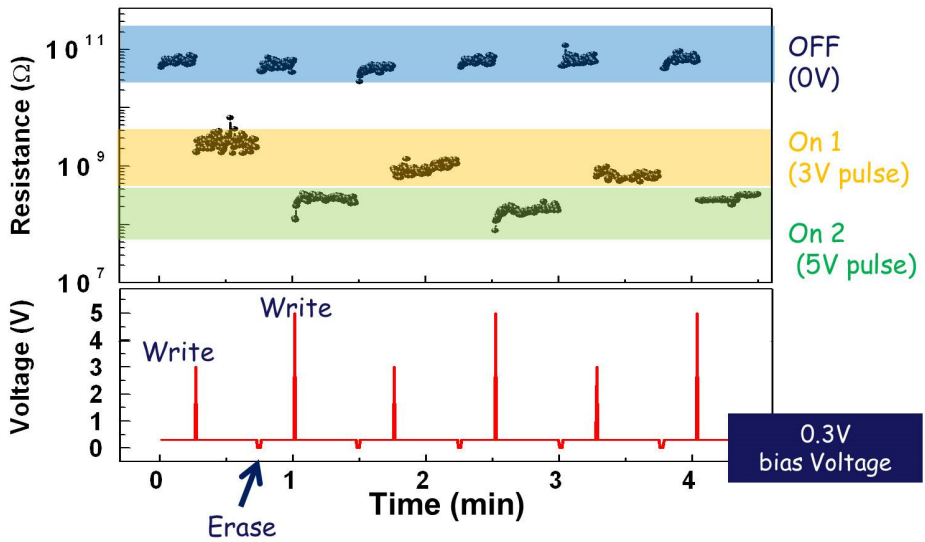


Figure 4-6 Demonstration of the information storage that shows reliable and non-volatile switching property of VO_2 single nanowire. The 0.3 V voltage bias is applied for reading, and the 3 and 5 V voltage pulses are applied for writing. The zero voltage is used for erasing and resetting to initial resistance.

4.4 Summary

In summary, in order to demonstrate a two-terminal memristor for next-generation non-volatile memory, the non-volatile switchable resistance of a single VO₂ nanowire, which was synthesized by hydrothermal process and thermal annealing, was investigated. The retainable and switchable resistance characteristics with wide range of accessible resistance can be successfully controlled with low voltage. This characteristic is connected with the percolative nature of the MIT; the mixed state of metallic and insulating phases in VO₂ material. The low voltage bias can maintain the resistances in the entire temperature range where MIT occurs due to the self-Joule heating. The self-Joule heating can bring accessible resistance within a range of four orders and reliable switching characteristic over 1 order of magnitude of resistance change. By applying zero bias voltage, the resistance can be reset to the initial insulating state. The resistivity changes for writing with voltage pulse and erasing with zero bias voltage show very high reproducibility. This is the first report of the memristor based on a single VO₂ nanowire. And also it is the first report of a simple two-terminal memristor which can be operated by voltage source without using any additional heating source; voltage pulse, bias voltage, zero bias voltage for writing, reading, and erasing, respectively, with retainable resistance. The development of a switch memory device based on VO₂ nanowire which can be operated by voltage source can open perspectives for low

power consumption, low cost fabrication process, high density and high performance with reliable and non-volatile switching characteristics in the memristor applications.

4.5 References

- [1] M. H. Kryder , C. S. Kim, *After Hard Drives-What Comes Next?*, IEEE Trans. Magn. 45 (2009) 3406–3413 .
- [2] L. O. Chua , *Memristor-The Missing Circuit Element*, IEEE Trans. Circuit Theory, 18 (1971) 507–519.
- [3] J. J. Yang , M. D. Pickett , X. Li , A. A. OhlbergDouglas , D. R. Stewart , R. S. Williams, *Memristive switching mechanism for metal/oxide/metal nanodevices*, Nat. Nanotechnol. 3 (2008) 429–433 .
- [4] M. K. Hota , M. K. Bera , B. Kundu , S. C. Kundu , C. K. Maiti, *A Natural Silk Fibroin Protein-Based Transparent Bio-Memristor*, Adv. Funct. Mater. 22 (2012) 4493–4499 .
- [5] F. Meng , L. Jiang , K. Zheng , C. F. Goh , S. Lim , H. H. Hng , J. Ma , F. Boey , X. Chen, *Protein-Based Memristive Nanodevices*, Small. 7 (2011) 3016–3020 .
- [6] D. B. Strukov , G. S. Snider , D. R. Stewart , R. S. Williams, *The missing memristor found*, Nature, 453 (2008) 80–83.
- [7] V. Erokhin , M. P. Fontana, *Electrochemically controlled polymeric device : a memristor (and more) found two years ago*, arXiv. (2008) arXiv:0807.0333.
- [8] S. H. Jo , T. Chang , I. Ebong , B. B. Bhadviya , P. Mazumder , W. Lu, *Nanoscale Memristor Device as Synapse in Neuromorphic Systems*, Nano Lett. 10

(2010) 1297–1301 .

[9] P. Krzysteczko , X. Kou , K. Rott , A. Thomas , G. Reiss, Current induced resistance change of magnetic tunnel junctions with ultra-thin MgO tunnel barriers, *J. Magn. Magn. Mater.* 321 (2009) 144–147 .

[10] P. Krzysteczko , G. Reiss , A. Thomas , Memristive switching of MgO based magnetic tunnel junctions, *Appl. Phys. Lett.* 95 (2009) 112508.

[11] T. Driscoll , H.-T. Kim , B.-G. Chae , B.-J. Kim , Y.-W. Lee , N. M. Jokerst , S. Palit , D. R. Smith , M. Di Ventra , D. N. Basov , Memory Metamaterials, *Science.* 325 (2009) 1518–1521 .

[12] T. Driscoll , H.-T. Kim , B.-G. Chae , M. Di Ventra , D. N. Basov , Phase-transition driven memristive system, *Appl. Phys. Lett.* 95 (2009) 043503 .

[13] H. Coy , R. Cabrera , N. Sepúlveda , F. E. Fernández , *Optoelectronic and all-optical multiple memory states in vanadium dioxide*, *J. Appl. Phys.* 108 (2010) 113115 .

[14] L. Pellegrino , N. Manca , T. Kanki , H. Tanaka , M. Biasotti , E. Bellingeri , A. S. Siri , D. Marré , *Multistate Memory Devices Based on Free-standing VO₂/TiO₂ Microstructures Driven by Joule Self-Heating*, *Adv. Mater.* 24 (2012) 2929–2934 .

[15] F. J. Morin , *Oxides Which Show a Metal-to-Insulator Transition at the Neel Temperature*, *Phys. Rev. Lett.* 3 (1959) 34–36 .

- [16] N. F. Mott , *Metal-Insulator Transition*, Rev. Mod. Phys. 40 (1968) 677–683 .
- [17] J. B. Goodenough , *The two components of the crystallographic transition in VO₂*, J. Solid St. Chem. 3 (1971) 490–500 .
- [18] M. Marezio , D. B. McWhan , J. P. Remeika , P. D. Dernier , *Structural Aspects of the Metal-Insulator Transitions in Cr-Doped VO₂*, Phys. Rev. B. 5 (1972) 2541–2551 .
- [19] A. Leitenstorfer , C. Kübler , R. Lopez , A. Halabica , R. F. Haglund , R. Huber, *Ultrafast insulator-metal transition in VO₂ : interplay between coherent lattice motion and electronic correlations*, Phys. Stat. Sol. C. 6 (2009) 149–151 .
- [20] C. Tang , P. Georgopoulos , M. E. Fine , J. B. Cohen , M. Nygren , G. S. Knapp , A. Aldred , *Local atomic and electronic arrangements in W_xV_{1-x}O₂*, Phys. Rev. B. 31 (1985) 1000–1011.
- [21] J. B. MacChesney , H. J. Guggenheim, *Growth and electrical properties of vanadium dioxide single crystals containing selected impurity ions*, J. Phys. Chem. Solids. 30 (1969) 225–234 .
- [22] H. Koo , S. Yoon , O.-J. Kwon , K.-E. Ko , D. Shin , S.-H. Bae , S.-H. Chang , C. Park , *Effect of lattice misfit on the transition temperature of VO₂ thin film*, J. Mater. Sci. 47(17) (2012) 6397–6401 .
- [23] K. Y. Tsai , T. S. Chin , H. P. D. Shieh , C. H. Ma, *Effect of as-deposited residual stress on transition temperature of VO₂ thin films*, J. Mater. Res. 19 (2004)

2306–2314.

[24] J. Cao , E. Ertekin , V. Srinivasan , W. Fan , S. Huang , H. Zheng , J. W. L. Yim , D. R. Khanal , D. F. Ogletree , J. C. Grossmanan , J. Wu , *Strain engineering and one-dimensional organization of metal-insulator domains in single-crystal vanadium dioxide beams*, Nat. Nanotechnol. 4 (2009) 732–737 .

[25] B. Hu , Y. Zhang , W. Chen , C. Xu , Z. L. Wang , *Self-heating and External Strain Coupling Induced Phase Transition of VO₂ Nanobeam as Single Domain Switch*, Adv. Mater. 23 (2011) 3536–3541 .

[26] B. Hu , Y. Ding , W. Chen , D. Kulkarni , V. V. Tsukruk , Z. L. Wang, *External-Strain Induced Insulating Phase Transition in VO₂ Nanobeam and Its Application as Flexible Strain Sensor*, Adv. Mater. 22 (2010) 5134–5139 .

[27] M. Wei , H. Sugihara , I. Honma , M. Ichihara , H. Zhou , *A New Metastable Phase of Crystallized V₂O₄ • 0.25H₂O Nanowires : Synthesis and Electrochemical Measurements*, Adv. Mater. 17 (2005) 2964–2969.

[28] J. Shi , S. Zhou , B. You , L. Wu , *Preparation and thermochromic property of tungsten-doped vanadium dioxide particles* ,Sol. Energy Mater. Sol. Cells. 91 (2007)1856–1862 .

[29] L. Dai , C. Cao , Y. Gao , H. Luo , *Synthesis and phase transition behavior of undoped VO₂ with a strong nano-size effect* ,Sol. Energy Mater. Sol.Cells. 95 (2011) 712–715.

- [30] P. P. Boriskov , A. A. Velichko , G. B. Stefanovich , *Effect of electric field on the metal-insulator transition with the formation of superstructure* , Phys. Solid State. 46 (2004) 922–926 .
- [31] H. T. Kim , B. G. Chae , D. H. Youn , G. Kim , S. J. Lee , K. Kim , Y. S. Lim , K. Y. Kang , *Raman study of electric-field-induced first-order metal-insulator transition in VO₂-based devices*, Appl. Phys. Lett. 86 (2005) 242101 .
- [32] E. Strelcov , Y. Lilach , A. Kolmakov , *Gas Sensor Based on Metal-Insulator Transition in VO₂ Nanowire Thermistor*, Nano Lett. 9 (2009) 2322–2326 .
- [33] A. Sharoni , J. G. Ramirez , I. K. Schuller , *Multiple Avalanches across the Metal-Insulator Transition of Vanadium Oxide Nanoscaled Junctions*, Phys. Rev. Lett. 101 (2008) 026404 .
- [34] M. M. Qazilbash , M. Brehm , B. G. Chae , P. C. Ho , G. O. Andreev , B. J. Kim , S. J. Yun , A. V. Balatsky , M. B. Maple , F. Keilmann , H. T. Kim , D. N. Basov , *Mott Transition in VO₂ Revealed by Infrared Spectroscopy and Nano-Imaging* , Science. 318 (2007) 1750–1753 .
- [35] A. Tselev , J. D. Budai , E. Strelcov , J. Z. Tischler , A. Kolmakov , S. V. Kalinin, *Electromechanical Actuation and Current-Induced Metastable States in Suspended Single-Crystalline VO₂ Nanoplatelets*, Nano Lett. 11 (2011) 3065–3073

Chapter 5. The memristive gas sensor based on a single VO₂ nanowire

5.1 Introduction

The sensor using semiconducting nanowire was based on the charge transfer mechanism between a nanowire surface and an analyte molecule followed by formation of charge-induced depletion/accumulation layer at nanowire surface^[1,2,3,4,5,6,7]. Since for thin enough nanowires, the radius and the width of the depleted layer are comparable, the adsorption/desorption of gas molecules effectively modulates the cross section of the nanowire which can act as the conducting channel.^[8,9]

A superconducting transition-edge sensor (TES), also called a superconducting phase-transition thermometer, consists of a superconducting film operated in the narrow temperature region between the normal and superconducting state, where the electrical resistance varies between zero and its normal value.^[10] A TES can be used in ultra-sensitive gas sensor. In these resistive type devices, the active sensing

element is made of superconducting material whose operating temperature is set to an extremely narrow region (transition edge) between superconductive and normal states. Thus, tiny variations of the sensor's temperature due to change of gas conditions like pressure, concentration and kinds of molecules will result in a drastic change of the resistance. This ultra-sensitivity of a TES makes it possible in principle transition to develop thermal detectors with faster response, larger heat capacity, and smaller detectable energy input than thermal detectors made using conventional semiconductor sensor.^[8,11]

However, the usage of superconducting sensing elements is experimentally demanding and expensive since it requires cryogenic temperatures. On the other hand, VO₂ is an actively studied strongly correlated oxide that exhibits a temperature driven metal-to-insulator transition (MIT) at ~ 68 °C in the bulk form where conductivity of the sample increases several orders of magnitude. The transition is accompanied by a crystalline structure change from monoclinic at low temperature insulating phase to a tetragonal one in a metal state. This sharp change in conductivity of VO₂ has been proposed as a working principle for uncooled TES microbolometers and critical temperature sensors. Table 5-1 showed the gas sensor performance of some 1-D oxide gas sensor.^[12,13,14,15,16]

The VO₂ gas sensors measured the transition voltage which can be different with the kind of gas or the pressure of gas around VO₂ materials.^[8,9] But in this case, the

one-off operation is one of critical disadvantage to deploy on a commercial scale. The one-off operation means that cooling time is necessary to return to the insulating initial state after transition voltage measurement. In previous results, the response time of VO₂ takes over 5 min because of this cooling time.^[9] This long response time is critical problem to realize the gas sensor with the real time measurement solved.

The memristive gas sensor is one of innovative solution for the long response time problem. The VO₂ gas sensors is operated by measurement of transition voltage which is triggering from insulating phase to metallic phase, while the memristive gas sensor can be operated by using a part of transition between the mixed states. In chapter 4, many mixed state that has various resistance state can be generated by controlling the voltage pulse. Because the cooling time is not needed to trigger another transition, the response time can be shorted. And the selectivity and sensitivity can be improved due to the repeated analysis is provided. Figure 5-1 shows the difference between the VO₂ gas sensor and the memristive gas sensor. In this chapter, in order to confirm the possibility of a memristive gas sensor, the effect of the gas pressure on the non-volatile switchable resistance of a single VO₂ nanowire is investigated

Materials	Sensor type	Sensitivity	Concentration	Response time	Reference
SnO ₂ nanobelt	FET	0.17	0.2%	N/A	12
SnO ₂ nanowire + Pd nanodot	FET	4	1ppm	~50s	13
ZnO nanorod	Resistor	0.04	200ppm	30-40s	14
VO ₂ nanowire + Pd nanodot	Resistor	1000	100%	~5min	15
WO _{2.72} nanowire	Resistor	22	1000ppm	40s	16

The target gas was hydrogen gas, and sensitivity is the change of resistance over the resistance ($S = \Delta \text{resistance} / \text{resistance}$)

Table 5-1 Gas sensor performance of some 1-D oxide gas sensor^[12,13,14,15,16]

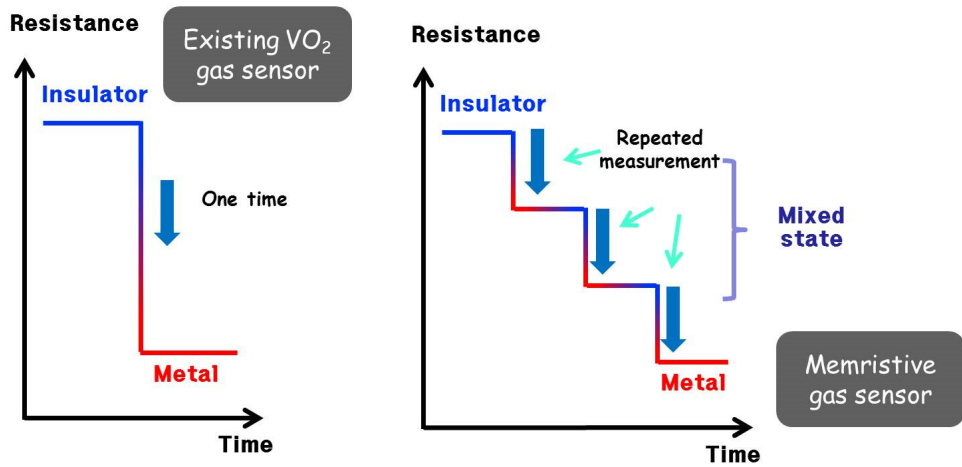


Figure 5-1 The different operation systems between the VO₂ gas sensor and the memristive gas sensor.

5.2 Experimental procedure

In order to investigate the memristive properties, a single nanowire with length and thickness of $\sim 30 \mu\text{m}$ and $\sim 160 \text{ nm}$, respectively, was connected to the silver electrodes on slide glass. For the memristive properties of single VO_2 nanowire, switchable and retainable resistance is needed.^[17] First, in order to confirm the potential of the retainable resistance, the I-V curve of the single nanowire in various pressures was obtained by measuring the change of resistance with the bias voltage. The memristive behavior of the single VO_2 nanowire was confirmed by observing the switching and non-volatile properties of resistances when voltage pulses and low bias voltage were applied, respectively. Furthermore, multiple retainable resistances can be utilized by controlling the number and the amount of voltage pulses under the low bias voltage. In order to confirm the possibility of a memristive gas sensor, the effect of the gas pressure on the non-volatile switchable resistance of a single VO_2 nanowire is investigated. The resistance change in mixed state is measured at various pressures.

5.3 Results & discussion

The effect of pressure on memritive properties of the single VO₂ nanowire was investigated for gas sensor application. Non-volatile resistance can be stabilized by bias voltage which can be determined from the transition voltage in I-V curve. To determine the bias voltage, I-V curves was measured in various pressures. Figure 5-2 showed the I-V curve of single VO₂ nanowire in 760Torr, 1Torr and 40mTorr. As the applied voltage increased, the Joule heating which was generated in VO₂ nanowire also increased. The temperature of nanowire raised and reach to the transition temperature, and the insulating VO₂(M) transited to the metallic VO₂(R). The Joule heat, released in the nanowire was used to trigger MIT directly. The resistance of the VO₂ nanowire was reduced with the bias voltage at room temperature by ~4 orders of magnitude upon the transition. Under applied voltage, the nanowire acts as a preheated thermistor whose temperature (and thus resistance) depends on the delicate balance between the incoming Joule heat and outgoing heat fluxes.^[18,19] The former is manipulated through the DC bias ramps, whereas the latter ones are determined mainly by the type of the ambient gas, its temperature, pressure, and heat dissipation into the metal contacts. Thus, any variations in the thermal conductivity of the ambient gas will be recorded as shifts in the transition voltage for MIT. When the pressure decreased, the heat desorption from the nanowire to the ambient gas molecules also decreased. So the transition voltage is

lower as decreasing the ambient gas pressure.

In order to investigate the effect of pressure on memritive properties, the change of resistance was measured with the number of voltage pulses of a single VO₂ nanowire. Figure 5-3 showed the change of resistance with voltage pulses in 760Torr and 1mTorr. Before applying the voltage pulses, the VO₂ nanowire was in the insulating state which has a resistance of $\sim 10^{12}\Omega$. When the voltage pulse was applied to the single nanowire, the resistance dropped to lower value due to the partial formation of the metallic phase in the insulating phase. The resistance decreases in a step-by-step mode corresponding to the application of repeated voltage pulses and the resistance is saturated to the value of $\sim 10^7\Omega$, which is the same as that of the metallic phase. When same voltage pulse applied to the nanowire, as the pressure decreased, the resistance of nanowire changed more lower value in mixed state from same resistance. If the resistance was same, the generated heat in the nanowire was also same. But due to the different pressure, the heat desorption from the nanowire to the ambient gas molecules was changed. The heat desorption in 1mTorr is smaller than that in 760Torr, the resistance drop was larger in 1mTorr. This show the possibility of a memristive gas sensor which ca detect the gas pressure by using the resistance change in mixed state.

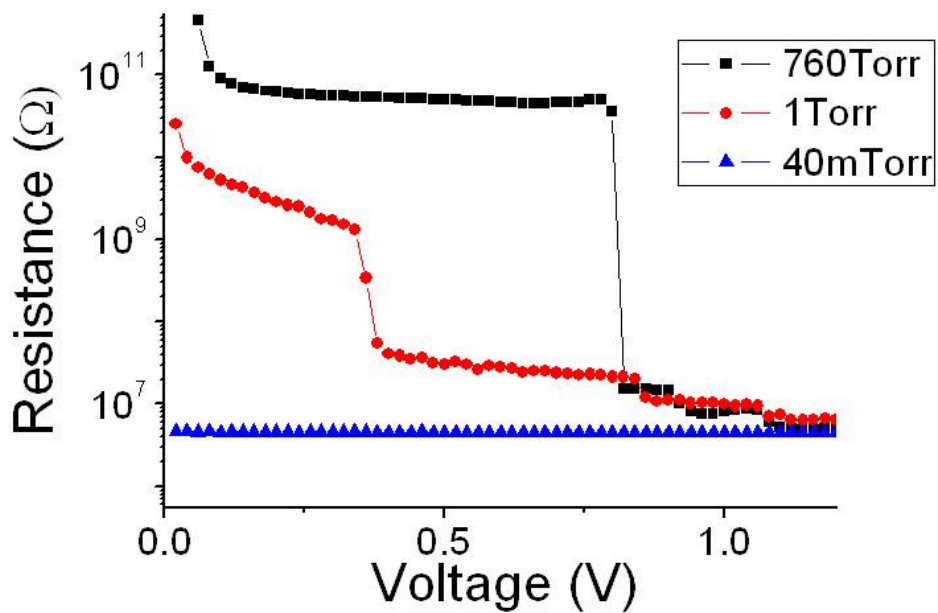


Figure 5-2 Resistance with bias voltage of annealed VO₂ nanowires in 760Torr (square), in 1Torr (circle), and in 40mTorr (triangle).

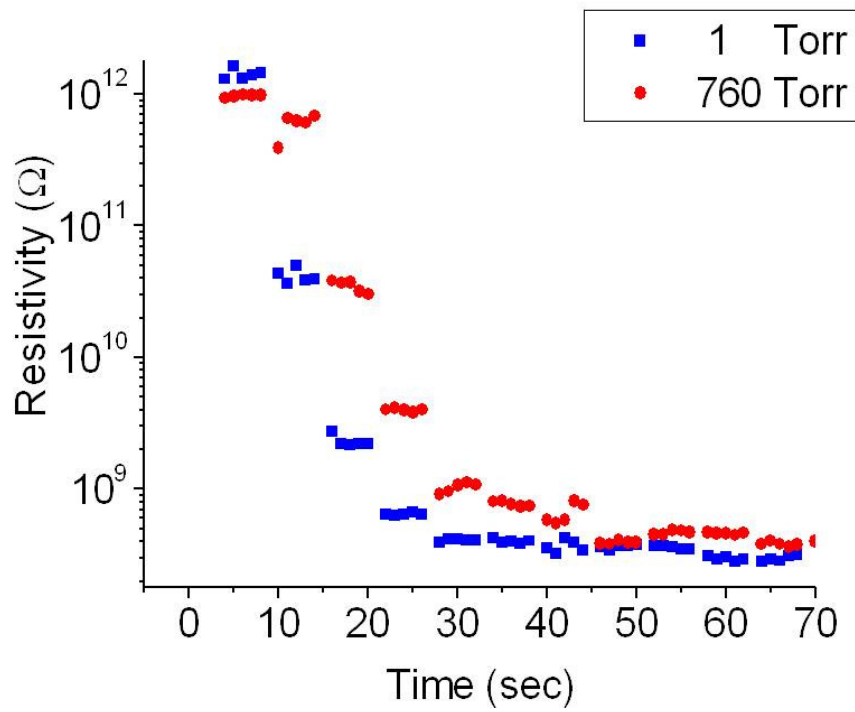


Figure 5-3 The change of resistance measured with 2V voltage pulses of a single VO₂ nanowire in 760Torr and 1Torr.

5.4 Summary

The memristive gas sensor is one of innovative solution for the long response time problem of the gas sensor based on MIT of VO₂. The VO₂ gas sensors is operated by measurement of transition voltage which is triggering from insulating phase to metallic phase. While the memristive gas sensor can be operated by using a part of transition between the mixed states. It provided fast response, repeatable measurement, improved sensitivity. In order to confirm the possibility of a memristive gas sensor, the effect of the gas pressure on the non-volatile switchable resistance of a single VO₂ nanowire is investigated. The VO₂ nanowire was connected electrically by using silver contact. The MIT of a single VO₂ nanowire can be successfully controlled by self-Joule heating without additional heating source. Non-volatile resistive memory can be stabilized by bias voltage which can be determined from the transition voltage in I-V curve. Due to the different pressure, the heat desorption from the nanowire to the ambient gas molecules was changed. As the pressure decreased, the transition voltage decreased, and the resistance of nanowire changed lower value in mixed state.

5.5 References

- [1] F. Patolsky, G. F. Zheng, C. M. Lieber, *Nanowire-Based Biosensors*, *Anal. Chem.* 78 (2006) 4260–4269.
- [2] P. C. Chen, G. Z. Shen, C. W. Zhou, *Chemical sensors and electronic noses based on one-dimensional metal oxide nanostructures*, *IEEE Trans Nanotechnol.* 7 (2008) 668–682.
- [3] E. Comini, C. Baratto, G. Faglia, M. Ferroni, A. Vomiero, G. Sberveglieri, *Quasi-one dimensional metal oxide semiconductors : Preparation, characterization and application as chemical sensors*, *Prog. Mater. Sci.* 54 (2009) 1–67.
- [4] A. Kolmakov, *Some recent trends in the fabrication, functionalisation and characterisation of metal oxide nanowire gas sensors*, *Int. J. Nanotechnol.* 5 (2008) 450–474.
- [5] S. J. Pearton, B. J. Kang, B. P. Gila, D. P. Norton, O. Kryliouk, F. Ren, Y. W. He, C. Y. Chang, G. C. Chi, W. M. Wang, L. C. Chen, *GaN, ZnO and InN Nanowires and Devices*, *Nanosci. Nanotechnol.* 8 (2008) 99–110.
- [6] A. Kolmakov, X. H. Chen, M. Moskovits, *Functionalizing Nanowires with Catalytic Nanoparticles for Gas Sensing Application*, *J. Nanosci. Nanotechnol.* 8 (2008) 111–121.
- [7] M. Law, D. J. Sirbully, P. D. Yang, *Chemical sensing with nanowires using*

electrical and optical detection, *Int. J. Nanotechnol.* 4 (2007) 252–262.

[8] E. Strelcov, Y. Lilach, and A. Kolmakov, *Gas Sensor Based on Metal-Insulator Transition in VO₂ Nanowire Thermistor*, *Nano Lett.* 9 (2009) 2322–2326

[9] J. M. Baik, M. H. Kim, C. Larson, C. T. Yavuz, G. D. Stucky, A. M. Wodtke, and M. Moskovits, *Pd-Sensitized Single Vanadium Oxide Nanowires: Highly Responsive Hydrogen Sensing Based on the Metal-Insulator Transition*, *Nano Lett.* 9 (2009) 3980–3984

[10] K. D. Irwin, G. C. Hilton, *Transition-Edge Sensors*, *Cryogenic Particle Detection*, 99 (2005) 63–149.

[11] J. Wei, D. Olaya, B. S. Karasik, S. V. Pereverzev, A. V. Sergeev, M. E. Gershenson, *Ultrasensitive hot-electron nanobolometers for terahertz astrophysics*, *Nat. Nanotechnol.* 3 (2008) 496–500.

[12] Y. Cheng, P. Xiong, L. Fields, J. P. Zheng, R. S. Yang and Z. L. Wang, *Intrinsic characteristics of semiconducting oxide nanobelt field-effect transistors*, *Appl. Phys. Lett.* 89 (2006) 093114

[13] A. Kolmakov, D. O. Klenov, Y. Lilach, S. Stemmer, M. Moskovits, *Enhanced gas sensing by individual SnO₂ nanowires and nanobelts functionalized with Pd catalyst particles*, *Nano Lett.* 5 (2005) 667–673

[14] O. Lupana, G. Chai, L. Chowa, *Novel hydrogen gas sensor based on single ZnO nanorod*, *Microelectr. Eng.* 85 (2008) 2220–2225

- [15] J. M. Baik, M. H. Kim, C. Larson, C. T. Yavuz, G. D. Stucky, A. M. Wodtke, and M. Moskovits, *Pd-Sensitized Single Vanadium Oxide Nanowires: Highly Responsive Hydrogen Sensing Based on the Metal-Insulator Transition*, Nano Lett. 9 (2009) 3980–3984
- [16] C. S. Rout, G. U. Kulkarni and C. N. R. Rao, *Room temperature hydrogen and hydrocarbon sensors based on single nanowires of metal oxides*, J. Phys. D, 40 (2007) 2777–2782
- [17] S-H. Bae, S. Lee, H. Koo, L. Lin, B. H. Jo, C. Park and Z. L. Wang, *The memristive properties of a single VO₂ nanowire with switching controlled by self heating*, Adv. Mater. 25 (2013) 5098–5103
- [18] J. M. Baik, M. H. Kim, C. Larson, A. M. Wodtke, M. J. Moskovits, *Nanostructure-Dependent Metal-insulator Transitions in vanadium-Oxide Nanowires*, Phys. Chem. C. 112 (2008) 13328–13331.
- [19] E. Strelcov, S. Dmitriev, B. Button, J. Cothren, V. Sysoev, Kolmakov, *Evidence of the self-heating effect on surface reactivity and gas sensing of metal oxide nanowire chemiresistors*, A. Nanotechnology, 19 (2008) 355502

Chapter 6. Thermochromic properties of VO₂ and polymer composite for smart window application

6.1 Introduction

The further development of smart window is thermochromism smart window, which can automatically change only its infrared optical transmittance with temperature without consuming other extra energy.^[1,2,3,4] The term ‘thermochromic’ is generally used for referring both thermotropic and thermochromic. However, for convenience, thermochromic windows based on hydrogels and polymer blends will be called as thermotropic, whereas those based on oxide thin film will be called as thermochromic in this dissertation.

For a thermochromic smart window, the thermochromic material would be coated on the glass surface, and then it works due to the thermochromism of the coating layer. The change of optical properties with temperature is usually related to a structural phase change on passing through a critical temperature, T_c . At

temperature below T_c , the material is relatively transparent in visible light and infrared range. This allows most of the solar radiation to pass through the window maximizing the heating effect of the sunlight and blockbody radiation within the building, keeping the interior warm. At temperatures above T_c , the thermochromic coating becomes infrared reflective, preventing thermal radiation from excessively heating the building interior while remaining visually transparent, enabling the optimum use of natural light. Minimizing the use of internal lighting also reduces building maintenance costs.^[5]

Many materials have such switching properties, and some of them are summarized in Table 6-1.^[6,7] By far, Vanadium dioxide(VO_2) has been the most widely studied, since the early demonstration of resistivity switching in bulk by Morin.^[6] The near proximity of the transition temperature to room temperature, at 68°C , is the most important reason.

Various deposition methods such as magnetron sputtering, pulsed laser deposition, electron beam evaporation, and chemical vapor deposition, have been reported to be used to fabricate VO_2 film. In order to control the stoichiometry of the film, high vacuum and high temperature is needed which lead high cost. However, if VO_2 is to be used in application like structural glass and automobile glass, the cost is very critical issue. For this reason, hydrothermal process and solution-based process are one of the best methods to produce the VO_2 thermochromic window in view of

various advantages; Easy and relatively cheap process.

Wei et al. reported the synthesis method of the hydrate VO₂ nanowire for application in battery.^[8] The method to synthesize the hydrate VO₂ is using the VO₂ powder; the synthetic process was not complicated, and made no impurity phase in the final product. High quality single crystal VO₂ nanowire can show superior phase transition properties which can be represented as the sharp and abrupt change due to its crystalline perfectness. The thermochromic properties based on superior phase transition of VO₂ nanowire can be improved. In this chapter, to develop the thermochromic window using hydrothermal process and solution-based process the thermochromic properties of the VO₂ nanowire was investigated.



Figure 6-1. ThermoSEE thermotropic glazing. The off-state is shown on the left and the heated on-state is shown on the right. (Credit: F. Millett, Pleotint, USA.)^[8]

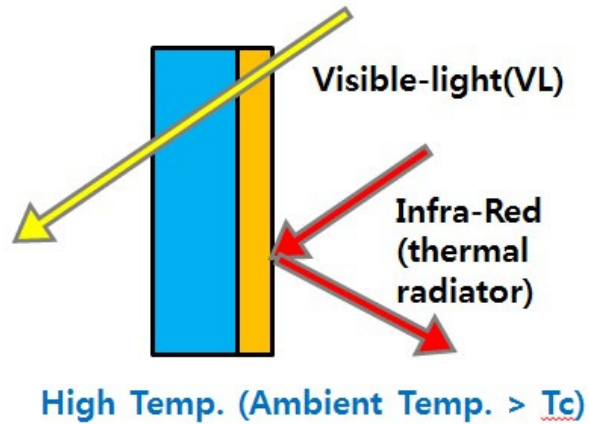
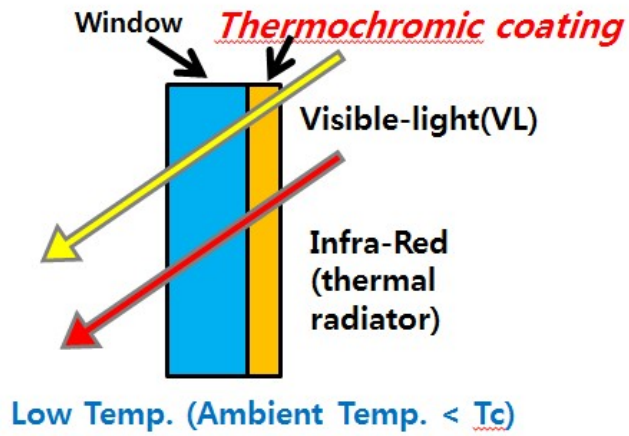


Figure 6-2 Schematic illustration of thermochromic smart window

Table 6-1. Comparison of various smart windows.

	Photo-chromic	Electro-chromic	Thermo-chromic
Source	Solar ray	Electric power	Heat
VIS Transparency	Changes Automatically	Changes Manually	Always Transparent
Operating Type	-	Manual	-
Weak Points	Not efficient during winter	Blocks VIS during Thermal Insulation	High IR Transmittance @High Temp.
Remarks	-	Requires Additional Energy	-

6.2 Experimental procedure

In order for VO₂ nanowires to be used in practical smart window applications, the thermochromic property of VO₂ nanowires and polymer composite was investigated. Colloidal VO₂ nanowires are fundamental materials of fast optical shutters for optical modulation and modulators in data storage and thermochromic coatings^[9]. The VO₂ nanowire does not form stable dispersions in organic solvents such as polyurethane. A second step is necessary that replaces surfacebound hexanoic acid with a surface-bonded, solvent-compatible, polymerizable material, (3-methacryloxypropyl)trimethoxysilane(MPTMS).^[10] Figure 6-3 showed the process of MPTMS treatment which was used in this thesis. After MPTMS treatment, VO₂ nanowires were dispersed in 2-butanone, forming a visually transparent colloid. For window application, the transmittance in visible light range should be improved. The antireflection coating is one of candidated method to improve the transmittance of the visible light, and by coating the VO₂ nanowire with SiO₂ layer as antireflection coating, cleared view can be achieved.^[11,12] VO₂ nanowire-SiO₂ core-shell nanostructure was fabricated by the silanization via hydrolysis of TEOS. VO₂ nanowires were first soaked into 0.5 M citric acid for 10 min to clean surface contaminations and modify the surface with citric groups. After rinsing with DI water and blow-drying with N₂, the nanowires were immersed into a homogeneous mixture composed of 30mL of EtOH, 4 mL of H₂O,

and 500 μL of TEOS for 20 min under stirring. Once 500 μL of ammonium hydroxide was added into the mixture, the reaction was initiated. The shell thickness was controlled by the hydrolysis time of TEOS after the accession of ammonium hydroxide. After reaction time, diluted water was added and the reaction was terminated. Figure 6-4 showed the process of TEOS treatment which was used in this thesis. The nanowire were removed from the reaction solution after a series of determined reaction time t , $t = 3, 5, 10, 30$ and 60min , followed by centrifugation, water rinsing and N_2 drying. All samples were stored in a vacuum chamber for further characterization. Colloid VO_2 nanowire and VO_2 - SiO_2 core-shell nanowires were dispersed in polyurethane and were deposited on fused silica substrate by the spin coating method. The thermochromic property was measured by FT-IR spectrophotometer in the wave number range $400\text{--}6000\text{cm}^{-1}$ with a programmable heating attachment. The spectra were collected at 20 and $80\text{ }^\circ\text{C}$, and at the fixed wavelength of 2000nm against temperature with a UV-vis spectrometer.

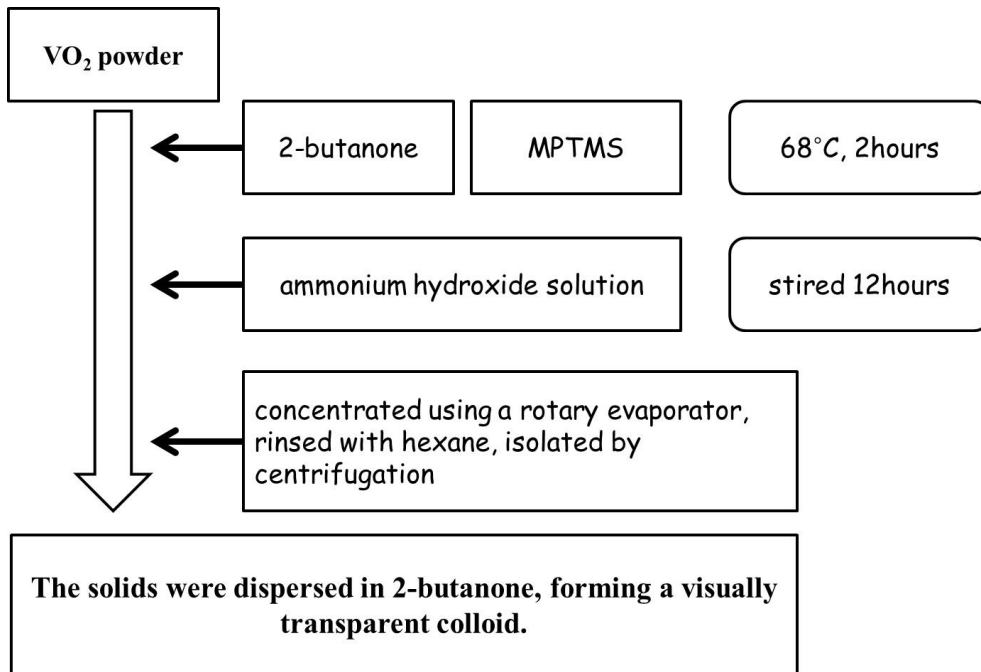


Figure 6-3 The step-by-step process of MPTMS treatment for dispersion

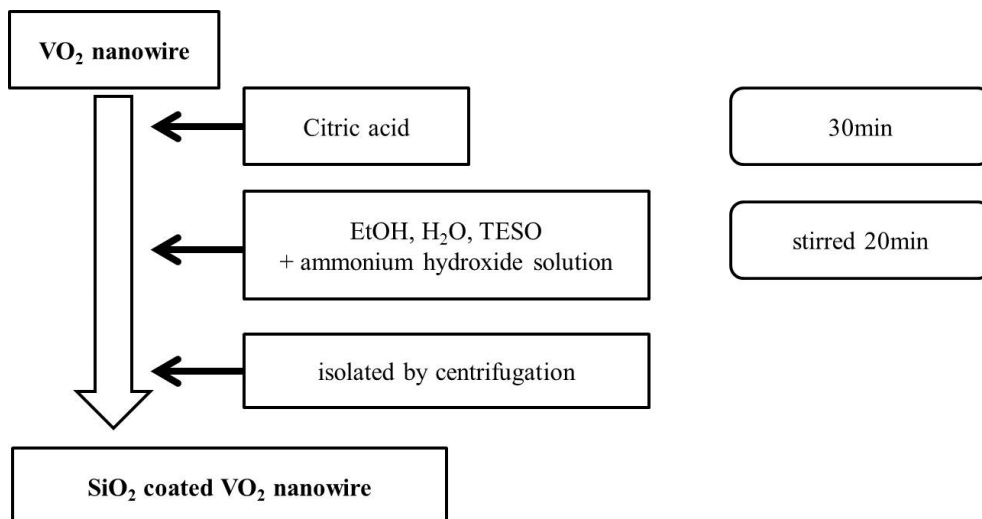


Figure 6-4 The step-by-step process of TEOS treatment to synthesize the VO₂-SiO₂ core-shell nanowire ^[13,14]

6.3 Results & discussion

The X-ray diffraction measurement was performed for phase identification of the nanowire. XRD pattern of the VO₂-SiO₂ core-shell nanowire (reaction time $t=5$ min) is depicted in Figure 6-5. XRD pattern shows intense Bragg diffraction peaks only from VO₂(M) phase which is agreement with the reported pattern(JCPDS 19-1398). No peaks of other phases or impurity was not observed. XRD pattern of the VO₂-SiO₂ core-shell nanowire (reaction time $t=30$ min) is depicted in Figure 6-6. It is notable that a broad peaks near $2\theta \approx 20 \sim 40^\circ$ from amorphous SiO₂ and very small intense Bragg diffraction peaks from VO₂(M) phase. Except amorphous peak, no peaks of other phases or impurity was not observed. In VO₂-SiO₂ core-shell nanowire (reaction time $t=30$ min), the thickness of SiO₂ layer is about 100um, so very small amount of X-ray can reach to the VO₂(M) phase.

Figure 6-7 shows DSC of the pure VO₂ nanowire and VO₂-SiO₂ core-shell nanowire. In heating cycle, the maximum peak position of VO₂ nanowire's exothermal peak is 58.11°C, and the half partial area position is 58.60°C. In cooling cycle, the maximum peak position of VO₂ nanowire's endothermal peak is 71.13°C, and the half partial area position is 71.85°C. The transition temperature of VO₂-SiO₂ core-shell nanowire is also similar with that of the pure VO₂ nanowire. It is notable that a VO₂-SiO₂ core-shell nanowire's transition is broader peak. It may

due to stress which can be created between VO₂ and SiO₂ during the structural change (VO₂(M)→VO₂(R) or VO₂(R)→ VO₂(M)).

In order to investigate the reaction time on SiO₂ thickness, the size of VO₂-SiO₂ core-shell nanowires was measured by the optical microscope. Figure 6-8 shows the microscope images of VO₂-SiO₂ core-shell nanowires which are followed the reaction; t = 5min and 30min. Figure 6-9 shows the graph and table which can show relationship between the reaction time and the thickness. As the TEOS process time increased, the thickness of SiO₂ layer also increased.

The actual nano-structure of VO₂-SiO₂ core-shell nanowire was confirmed by TEM analysis, as shown in Figure 6-10. VO₂-SiO₂ core-shell nanowire (t=5min). The VO₂-SiO₂ core-shell nanowire deposited on Si substrate and was cut by FIB. The sample size is 20um x 10um x 100nm. From high resolution TEM image (Figure 6-10(b)) and selected area electron diffraction pattern (Figure 6-10(c)), the nanowire was single crystal without any grain boundary. The VO₂ nanowire was coated uniformly by SiO₂, and the thickness of SiO₂ was ~100nm. There is no intense peak in electron diffraction pattern ((Figure 6-10(d)), SiO₂ was amorphous phase.

Figure 6-11 and 6-12 showed EDS mapping result. EDS showed the core nanowire is pure VO₂ and the capping layer is pure SiO₂. This showed the VO₂-SiO₂ core-shell nanowire successively synthesized.

Figure 6-13 showed the spectral transmittance of VO₂ nanowire + polyurethane composite deposited on fused silica. The concentration of the VO₂ nanowire + polyurethane composite was 20wt% (= 5volume% VO₂ nanowire / polyurethane). The spin coating was carried out for 20 times in (a) and (b), for 30 times in (c). The composite based on pure nanowire which was not treated any dispersion or coating showed very poor thermochromic properties (Figure 6-13(a)). When VO₂ nanowire was treated by MPTMS, the Infrared(IR) transmittance change(@λ=2500nm) was improved about 7%. The IR transmittance changes of the composited based on VO₂-SiO₂ core-shell nanowire, were larger than 20%. It was notable that the transmittance in visible light was higher when VO₂-SiO₂ core-shell nanowire used.

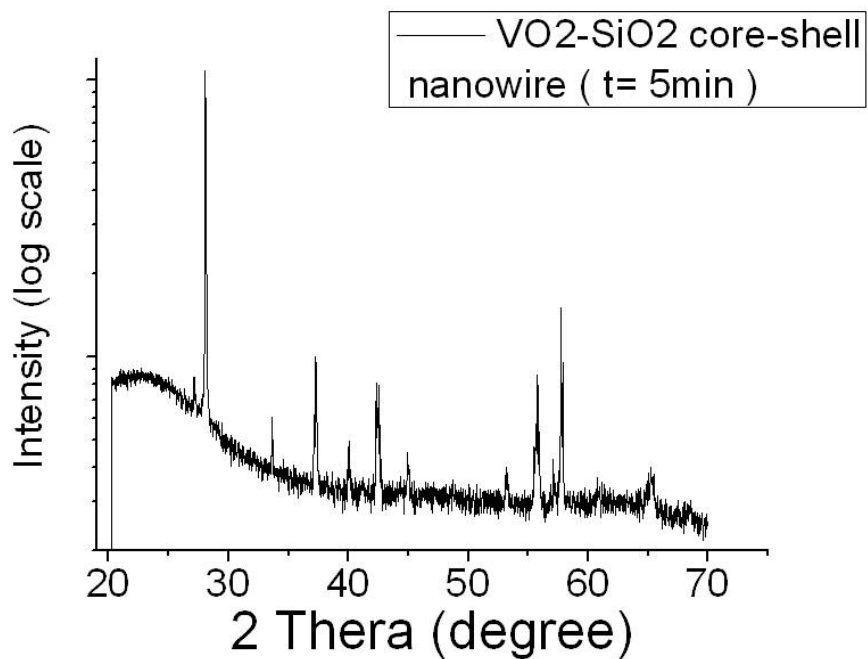


Figure 6-5 XRD diffraction pattern of VO₂-SiO₂ core-shell nanowire (t=5min)

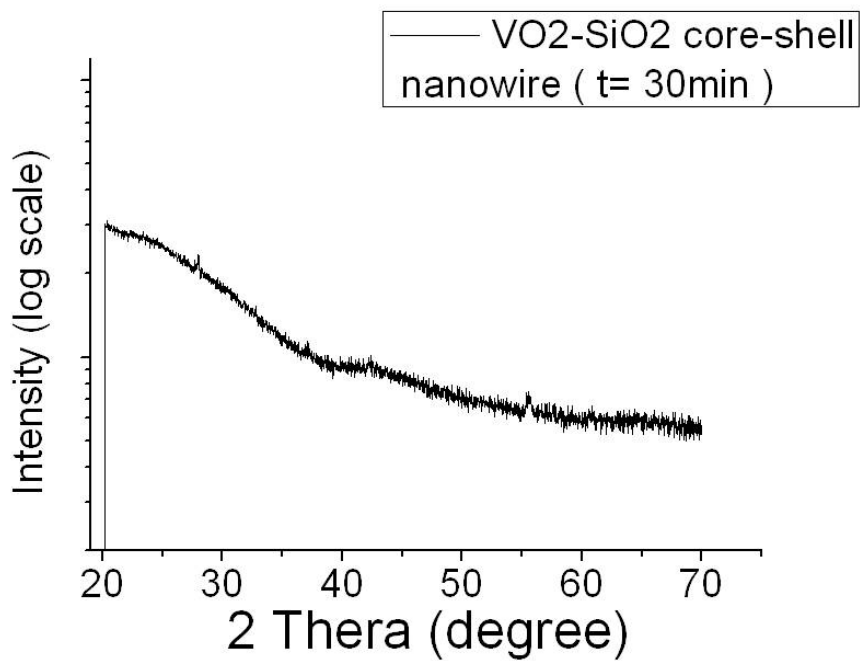


Figure 6-6 XRD diffraction pattern of VO₂-SiO₂ core-shell nanowire (t=30min)

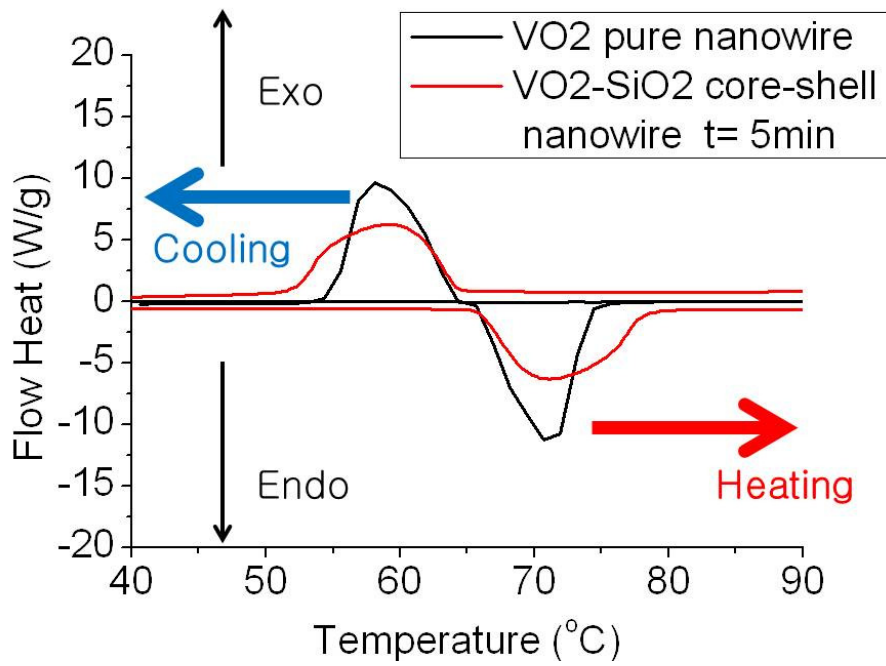


Figure 6-7 DSC results of the pure VO₂ nanowire and VO₂-SiO₂ core-shell nanowire.

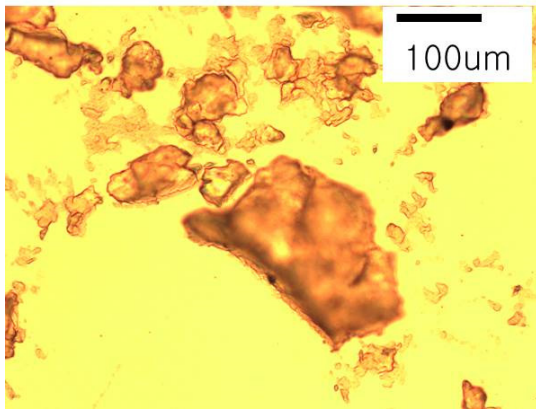
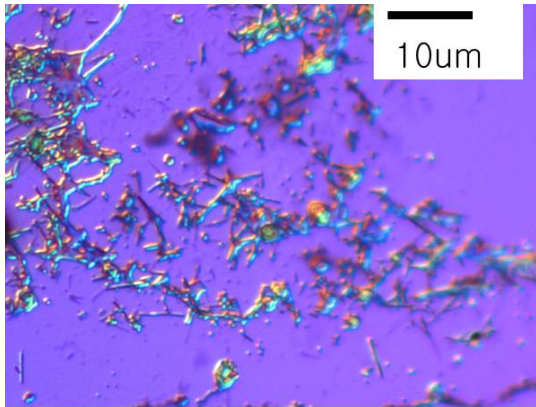


Figure 6-8 The microscope images of $\text{VO}_2\text{-SiO}_2$ core-shell nanowires which are followed the reaction; $t = 5\text{min}$ and 30min .

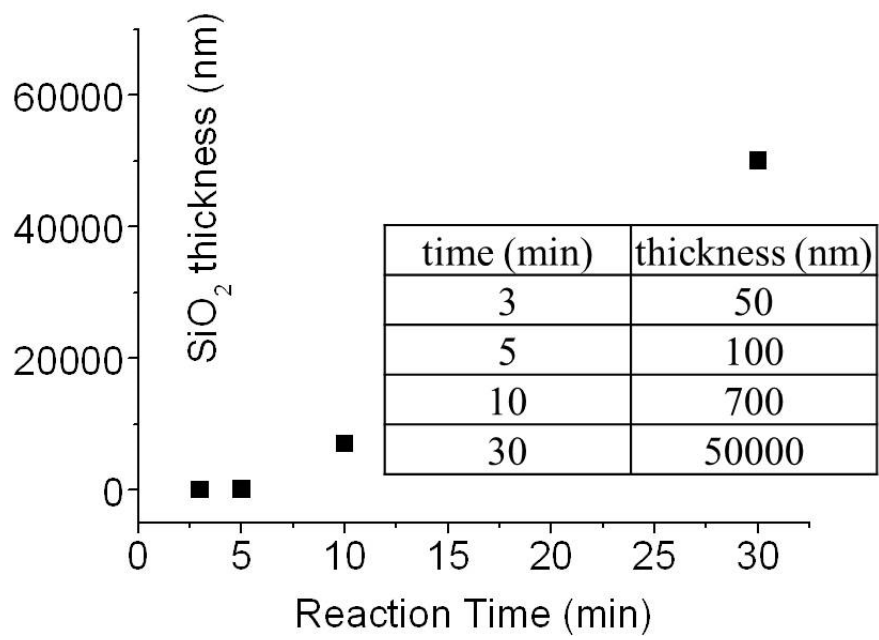


Figure 6-9 The graph and table which can show relationship between the reaction time and the thickness

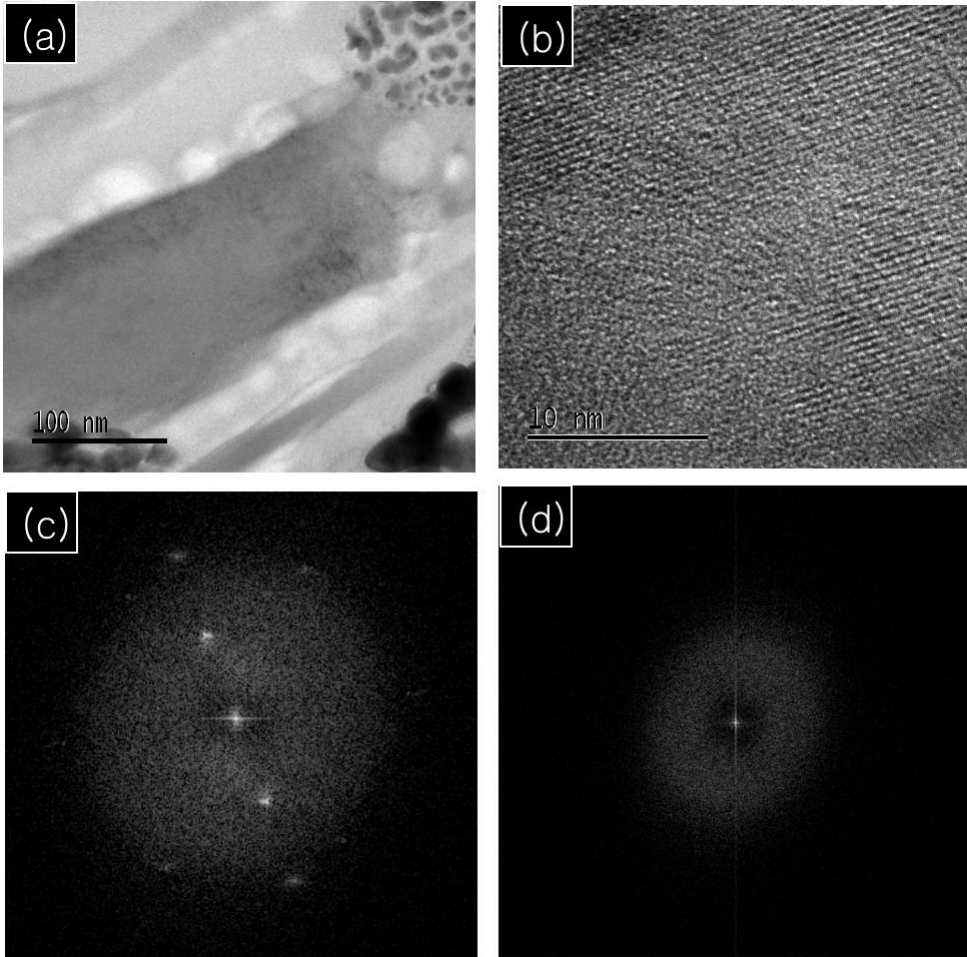


Figure 6-10 The actual nano-structure of VO₂-SiO₂ core-shell nanowire was confirmed by TEM analysis

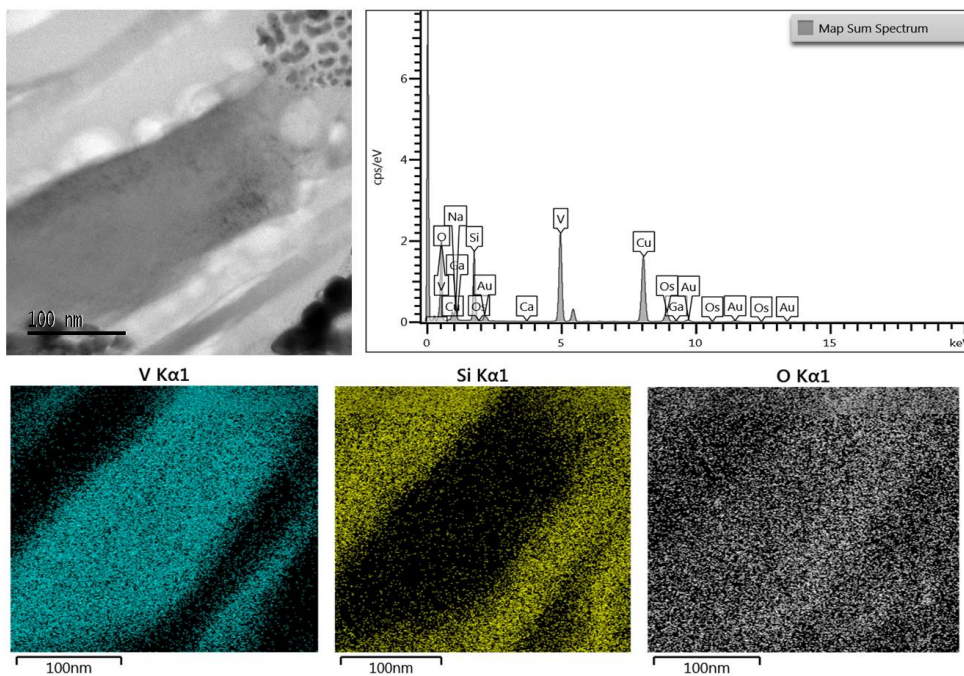


Figure 6-11 EDS mapping result of the $\text{VO}_2\text{-SiO}_2$ core-shell nanowire successively synthesized.

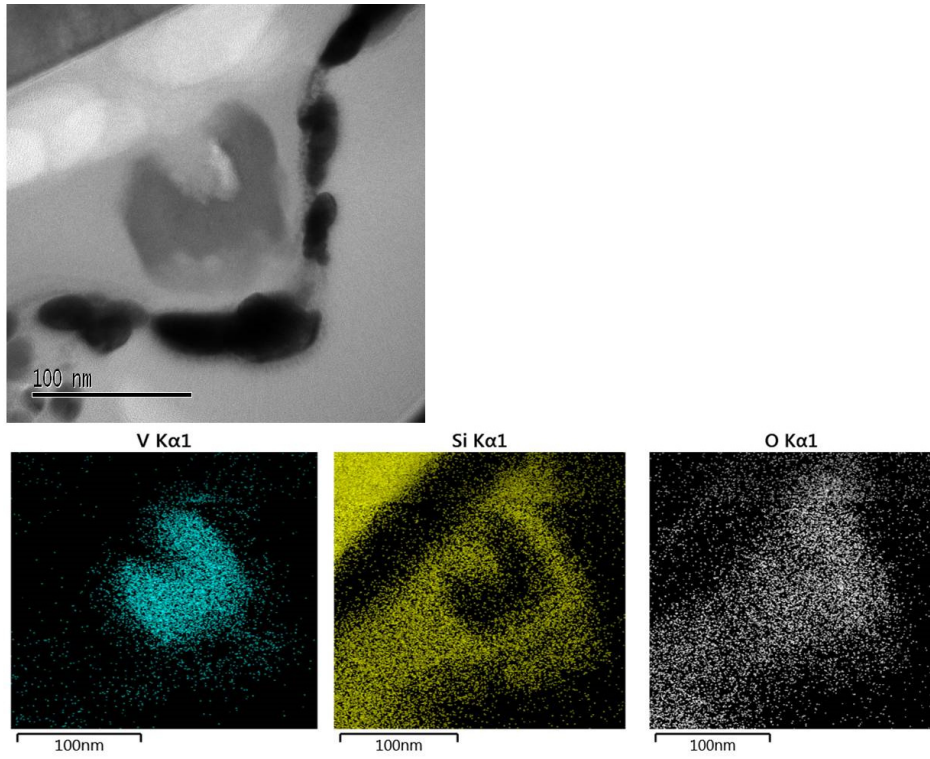


Figure 6-12 EDS mapping result of the VO₂-SiO₂ core-shell nanowire successively synthesized

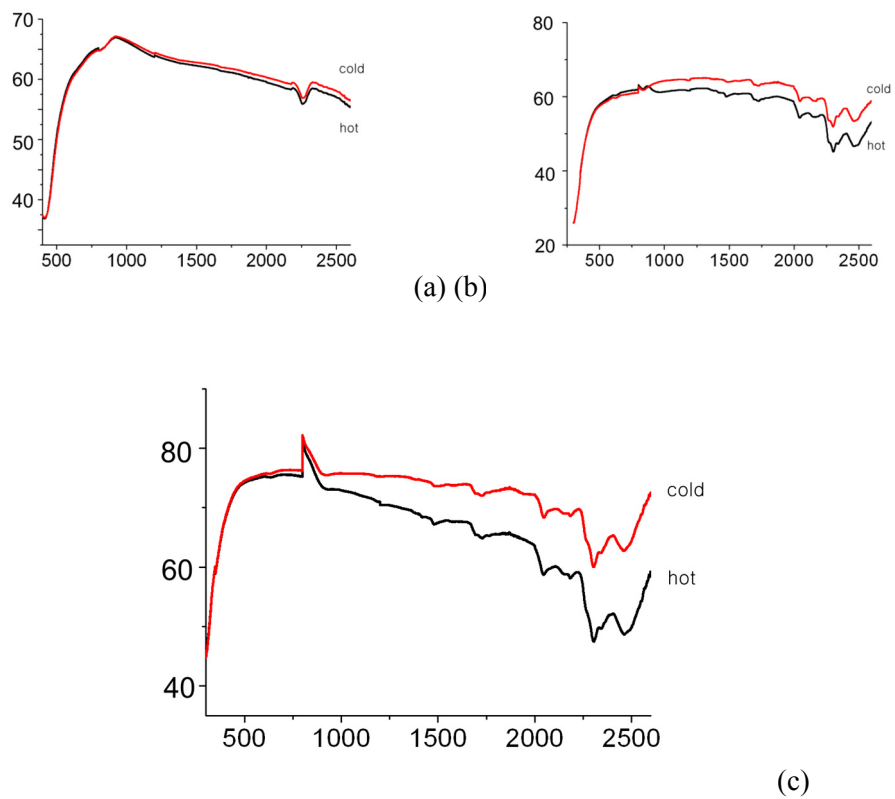


Figure 6-13 The spectral transmittance of VO₂ nanowire + polyurethane composite deposited on fused silica

6.4 Summary

In order to investigate the thermochromic properties of the VO₂ nanowire, VO₂ and polymer composites were deposited on fused silica substrate by the spin coating method. By using MPTMS treatment which could replace surfacebound hexanoic acid with a surface-bonded, the colloidal VO₂ nanowires were synthesized successfully. The VO₂ nanowire formed stable dispersions in organic solvents with a visually transparent colloid such as polyurethane. In order to improve the thermochromic property, the VO₂ nanowire was coated by SiO₂ layer as antireflection coating. VO₂-SiO₂ core-shell nanowire was fabricated by the silanization via hydrolysis of TEOS. The micro and nano structure of VO₂ nanowire-SiO₂ core-shell was investigated by the microscope, the FESEM and the TEM. As result of XRD and EDS, SiO₂ coating layer which has the thickness from 100nm to 100um was the amorphous silicon oxide. Colloid VO₂ nanowire and VO₂-SiO₂ core-shell nanowires were dispersed in polyurethane and were deposited on fused silica substrate by the spin coating method. The thermochromic property was measured by FT-IR spectrophotometer in the wave number range 400–6000cm⁻¹ with a programmable heating attachment. The thermochromic property was improved after MPTMS treatment and the transmittance in visible light was improved after SiO₂ antireflection coating. The IR transmittance changes of the composited based on VO₂-SiO₂ core-shell nanowire, are larger than 20%. It was

notable that the transmittance in visible light was higher when VO₂-SiO₂ core-shell nanowire used.

6.5 References

- [1] M. Soltani, M. Chaker, E. Haddad, and R.V. Kruzelesky, Thermochromic vanadium dioxide smart coatings grown on Kapton substrates by reactive pulsed laser deposition, *J. Vac. Sci. Technol. A* 24 (2006) 612
- [2] F. Guinneton, L. Sauque, J.C. Valmalette, F. Cros, and J.R. Gavarrri, Optimized infrared switching properties in thermochromic vanadium dioxide thin films: role of deposition process and microstructure, *Thin Solid Films* 446 (2004) 287
- [3] I. Takahashi et al., Thermochromic $V_{1-x}W_xO_2$ thin films prepared by wet coating using polyvanadate solutions, *Jpn. J. of Appl. Phys.* 35 (1996) 438
- [4] K. Kato, et al., Study on thermochromic VO_2 films grown on ZnO-coated glass substrates for “smart windows,” *Jpn. J. of Appl. Phys. Part 1- Regular Papers Short Notes Review Papers*, 42 (2003) 6523
- [5] I.P. Parkin and T.D. Manning, Intelligent thermochromic windows, *Journal of Chemical Education* 83 (2006) 393
- [6] F.J. Morin, Oxides which show a metal-to-insulator transition at the Neel temperature, *Phys. Rev. Lett.* 3 (1959) 34
- [7] C.M. Lampert, *Chromogenic smart materials*, *Materialstoday* (2004) 28
- [8] M. Wei , H. Sugihara , I. Honma , M. Ichihara , H. Zhou , *A New Metastable Phase of Crystallized $V_2O_4 \cdot 0.25H_2O$ Nanowires : Synthesis and Electrochemical*

Measurements, Adv. Mater. 17 (2005) 2964–2969

[9] Y. Gao, C. Cao, L. Dai, H. Luo, M. Kanehira, Y. Ding and Z. L. Wang, *Phase and shape controlled VO₂ nanostructures by antimony doping*, Energy Environ. Sci. 5 (2012) 8708

[10] Y. Q. Rao, B. Antalek, J. Minter, T. Mourey, T. Blanton, G. Slater, L. Slater, J. Fornalík, *Organic Solvent-Dispersed TiO₂ Nanoparticle Characterization*, Langmuir, 25 (2009) 12713

[11] G.Xu, et al., Optimization of antireflection coating for VO₂-based energy efficient window, Solar Energy Materials & Solar Cells 83 (2004) 29-37.

[12] H. Koo, D. Shin, S-H. Bae, K-E. Ko, S-H. Chang, and C. Park, *The effect of CeO₂ antireflection layer on the optical properties of thermochromic VO₂ film for smart window system*, Journal of Materials Engineering and Performance, 23 (2014) 402

[13] C. Song, J. Chen, J. L. Abell, Y. Cui, Y. Zhao, *Ag-SiO₂ core-shell nanorod arrays: morphological, optical, SERS, and wetting properties*. Langmuir. 28 (2011) 1488

[14] Y. Yin, Y. Lu, Y. Sun, and Y. Xia, *Silver Nanowires Can Be Directly Coated with Amorphous Silica To Generate Well-Controlled Coaxial Nanocables of Silver/Silica*, Nano Lett. 2 (2002) 427

Chapter 7. Summary and suggestions for future work

Vanadium dioxide (VO_2) nanowire was synthesized by hydrothermal process which was followed by thermal annealing in order to fabricate the devices and investigate the applicability of the devices which are based on metal-to-insulator transition. Figure 7-1 showed the strategy of this thesis to fabricate the nanodevices based on VO_2 nanowire. VO_2 provided the room temperature operation, high speed, and high performance due to the large and abrupt optical/electrical change. The nanowire could promise the self-Joule heating operation with low power consumption, the high device density (small size) and improved performance due to high surface/volume ratio. The hydrothermal process had advantage to high purity VO_2 with various nanostructure in fast and low cost process. This study could be a one of key to realize the practical application of VO_2

First, the hydrothermal process was performed with various conditions in order to investigate the effect of process time and temperature on the structure of the VO_2 nanowire. The VO_2 hydrate nanowires were formed after hydrating–exfoliating–splitting steps through the hydrothermal process, and each step was confirmed by the field emission scanning electron microscope (FESEM). As the process temperature increased, the nanowire became thinner. As the process time increased,

the nanowire became thinner, but the limit of a convergent of the diameter was about 60nm. In order to dehydrate the nanowires, thermal annealing at 400°C in N₂ atmosphere for 4 hours was carried out. XRD and DSC results showed that the nanowires were VO₂(M) without any hydrate phases and that the MIT occurred at ~68°C in a heating cycle. These results suggest that the new method to synthesize the pure VO₂(M) nanowires.

Second, in order to investigate the memristive properties of the VO₂ nanowire, the VO₂ nanowire was connected electrically by using silver contact. The MIT of a single VO₂ nanowire can be successfully controlled by self-Joule heating without additional heating source. Non-volatile resistive memory could be stabilized by bias voltage to read the resistance. Various resistance states could be achieved by efficient Joule heating that accompany with voltage pulse. The single VO₂ nanowire showed ~10⁴ accessible resistance range which was similar range between fully metallic and insulating state. And the resistance could change abruptly with voltage pulse. By thermal cooling with zero voltage, the nanowire could be reset to fully insulating state. The process of writing with voltage pulse and erasing with thermal cooling showed very high reproducibility in resistance. The VO₂ nanowire could be Non-volatile resistive memory could be stabilized by bias voltage to read the resistance. This is first report that the memristive system controlled by self Joule heating and the memristive properties of single VO₂

nanowire.

Third, the effect of pressure on memritive properties of the single VO₂ nanowire was investigated for gas sensor application. The MIT of a single VO₂ nanowire could be successfully controlled by self-Joule heating without additional heating source. Non-volatile resistive memory could be stabilized by bias voltage which can be determined from the transition voltage in I-V curve. When same voltage pulse applied to the nanowire, as the pressure decreased, the resistance of nanowire changed lower resistance value in mixed state. This is the first report of the memristive gas sensor.

Finally, in order for VO₂ nanowires to be used in practical smart window applications, the thermochromic property of VO₂ nanowires and polymer composite was investigated. By using MPTMS treatment which could replace surfacebound hexanoic acid with a surface-bonded, the colloidal VO₂ nanowires were synthesized successfully. The VO₂ nanowire formed stable dispersions in organic solvents with a visually transparent colloid such as polyurethane. In order to improve the thermochromic property, the VO₂ nanowire was coated by SiO₂ layer as antireflection coating. VO₂-SiO₂ core-shell nanowire was fabricated by the silanization via hydrolysis of TEOS. The micro and nano structure of VO₂ nanowire-SiO₂ core-shell was investigated by the microscope, the FESEM and the TEM. As result of XRD and EDS, SiO₂ coating layer which has the thickness from

100nm to 100um was the amorphous silicon oxide. Colloid VO₂ nanowire and VO₂-SiO₂ core-shell nanowires were dispersed in polyurethane and were deposited on fused silica substrate by the spin coating method. The thermochromic property was improved after MPTMS treatment and the transmittance in visible light was improved after SiO₂ antireflection coating. The IR transmittance changes of the composited based on VO₂-SiO₂ core-shell nanowire, are larger than 20%. It was notable that the transmittance in visible light was higher when VO₂-SiO₂ core-shell nanowire used.

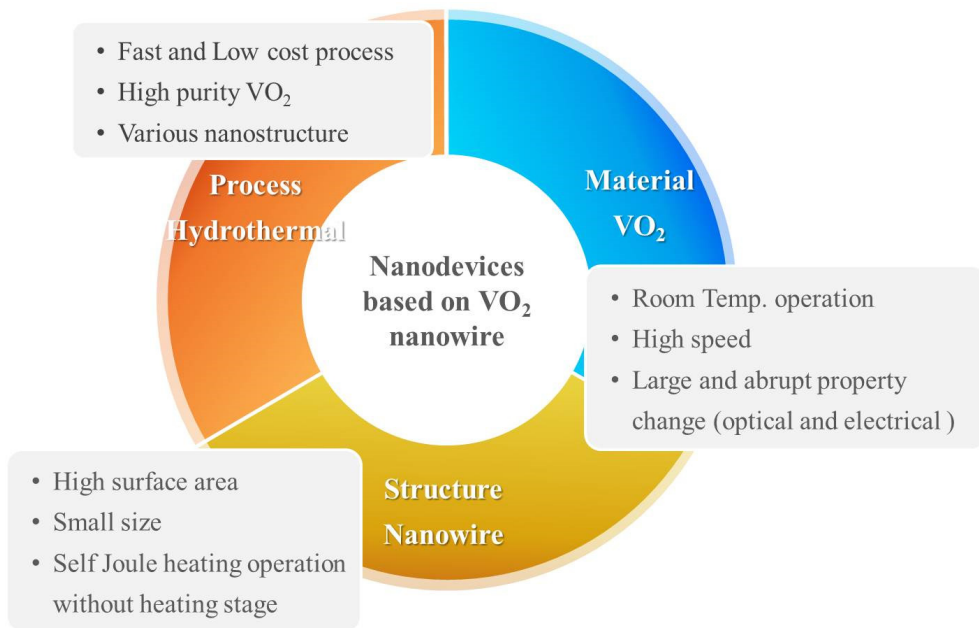


Figure 7-1 The strategy of this thesis to fabricate the nanodevices based on VO₂ nanowire

Publications

1. Sung-Hwan Bae, Sangmin Lee, Hyun Koo, Long Lin, Bong Hyun Jo, Chan Park and Zhong Lin Wang, " The memristive properties of a single VO₂ nanowire with switching controlled by self heating" *Advanced Materials*, 25, 5098-103 (2013)
2. Sangmin Lee, Sung-Hwan Bae, Long Lin, Ya Yang, Chan Park, Sang-Woo Kim, Seung Nam Cha, Hyunjin Kim, Young Jun Park, Zhong Lin Wang , “Super-Flexible Nanogenerator for Energy Harvesting from Gentle Wind and as an Active Deformation Sensor”, *Advanced Functional Materials*, 23, 2445–2449(2013)
3. Sangmin Lee, Sung-Hwan Bae, Long Lin, Seunghyun Ahn, Chan Park, Sang-Woo Kim, Seung Nam Cha, Young Jun Park, Zhong Lin Wang, “Flexible hybrid cell for simultaneously harvesting thermal and mechanical energies”, *Nano Energy*, 2, 817-825 (2013)
4. Sung-Hwan Bae, Il Hwan Yoo, Sukill Kang, and Chan Park, “The Effect of Tail State on the Electrical and the Optical Properties in Amorphous IGZO” *Journal of the Korean Ceramic Society*, 47, 329-332 (2010)
5. Sejin Yoon, O-Jong Kwon, Seunghyun Ahn, Jae-Yeol Kim, Hyun Koo, Sung-

Hwan Bae, Jun-Young Cho, Chan Park, “The Effect of Grain Size and Density on the Thermoelectric Properties of Bi₂Te₃-PbTe Compounds”, *Journal of Electronic Materials*, 45, 3390-3396 (2013)

6. Seunghyun Ahn, Hyun Koo, Sung-Hwan Bae, Chan Park, GuYoung Cho, IkWhang Chang, Suk-Won Cha, Young-Sung Yoo, “Effect of nickel contents on the microstructure of mesoporous nickel oxide/gadolinium-doped ceria for the anode of solid oxide fuel cells,” *Functional Materials Letters* , 6, 1350055 (2013)

7. Hyun Koo, Dongmin Shin, Sung-Hwan Bae, Kyeong-Eun Ko, Se-Hong Chang, and Chan Park, “The effect of CeO₂ antireflection layer on the optical properties of thermochromic VO₂ film for smart window system,” *Journal of Materials Engineering and Performance*, online published (2013)

8. Seunghyun Ahn, Hyun Koo, Sung-Hwan Bae, Ikwhang Chang, Sukwon Cha, Young-sung Yoo, and Chan Park, “The Grain Growth Behavior of NiO in Thermally-stable Mesoporous Gadolinium-doped Ceria Network for Intermediate Temperature SOFC Anode Materials,” *Journal of Nanoscience and Nanotechnology*, Submitted (2012)

9. Hyun Koo, Sejin Yoon, O-Jong Kwon, Kyeong-Eun Ko, Dongmin Shin, Sung-Hwan Bae, Se-Hong Chang, Chan Park, “Effect of lattice misfit on the transition temperature of VO₂ thin film,” *Journal of Material Science*, 47 (2012) 6397-6401

10. Il Hwan Yoo, Sung-Hwan Bae, Hyun Koo, O-Jong Kwon, Jaeun Yoo, Sukill Kang, Chan Park, "Electrical and Optical Properties of Amorphous (In,Sn)-Ga-Zn-O Thin Film," *Journal of Nanoscience and Nanotechnology*, 12 (2012) 3673-3676
11. Yung-Bin Chung, Sang-Hoon Lee, Sung-Hwan Bae, Hyung-Ki Park, Jae-Soo Jung, Nong-Moon Hwang, "Effect of the Initial Structure on the Electrical Property of Crystalline Silicon Films Deposited on Glass by Hot-Wire Chemical Vapor Deposition" *Journal of Nanoscience and Nanotechnology*, 12, 5947-5951 (2012)
12. O-Jong Kwon, Wook Jo, Kyeong-Eun Ko, Jae-Yeol Kim, Sung-Hwan Bae, Hyun Koo, Seong-Min Jeong, Jin-Sang Kim, Chan Park, "Thermoelectric properties and texture evaluation of $\text{Ca}_3\text{Co}_4\text{O}_9$ prepared by a cost-effective multisheet cofiring technique," *Journal of Materials Science*, 46 (2011) 2887-2894
13. Hyunwoo You, Sung-Hwan Bae, Jongman Kim, Jin-Sang Kim, Chan Park, Deposition of nano crystalline Bi_2Te_3 films using modified MOCVD system, *Journal of Electronic Materials*, 40(5), 635-540 (2011)
14. O-Jong Kwon, Jonglo Park, Ju-Hyuk Yim, Hyun Koo, Jae-Yeol Kim, HyunWoo You, Sung-Hwan Bae, Jin-Sang Kim, Chan Park, "The effect of microstructure on the thermoelectric properties of Bi_2Te_3 -PbTe alloy," *Current Applied Physics*, 11 (2011) S242-S245

15. Rock-Kil Ko, Sung-Hwan Bae, Myung-Jin Jung, Se-Hoon Jang, Kyu-Jeong Song, Chan Park, Myung-Hwan Sohn, Suk-Il Kang, Sang-Soo Oh, Dong-Woo Ha, Hong-Soo Ha, Ho-Sup Kim, Young-Cheol Kim, “Mixed Rare Earth (Nd_{1/3}Eu_{1/3}Gd_{1/3})Ba₂Cu₃O_{7-d} Thin Films by PLD for Coated Conductor”, IEEE Transactions on Applied Superconductivity 19(3), 3136-9 (2009)

국문 초록

이산화바나듐(VO_2)는 68도 부근에서 금속-절연체 상전이(MIT) 특성을 보이는 재료로, 상전이 시 급격한 저항 및 광학적 특성의 변화를 보이고, 그 전이 속도가 매우 빠르며, 상온 부근에서 전이온도를 가지는 특성을 보인다. 이러한 이산화바나듐의 전이특성을 이용하여 메모리소자, 스위치소자, 가스센서, 온도가변형 적외선 차단 소자, 광학 소자에 응용하려는 연구가 진행되고 있다.

이산화바나듐을 이용한 기존의 나노소자의 경우 박막구조의 이산화바나듐을 진공공정을 통하여 제작해 왔다 하지만 CVD, PVD와 같은 진공공정의 경우 높은 진공도와 온도를 요구한다는 점에서 공정비용이 증가하고, 기관에 선택에 있어 자유롭지 못한 단점을 가진다. 박막 형태의 이산화바나듐 소자의 경우 전이온도까지 소자온도를 올려줄 수 있는 발열체가 추가로 존재해야 하며, 높은 결정성을 얻기 위해서는 단결정 기관을 요구한다는 점도 실제 소자 응용에 있어 한계가 있다. 본 연구에서는 수열합성법으로 이산화바나듐 나노와이어를 제작하고 이를 응용하여 단순한 구조를 가지면서 저비용으로 소자제작이 가능한 나노소자를 제작하는 연구를 진행하였다.

수열합성법은 저비용으로 순수한 나노구조를 가지는 이산화바나듐을 제조할 수 있는 합성법으로 기존에 보고된 이산화바나듐 수화물 나노와이어를 제조하는 공정을 이용하여 순수한 이산화바나듐을 합성하였다. 수열합성법으로 제조된 이산화바나듐 수화물 나노와이어를 후열처리를 통하여 순수한 이산화바나듐을 합성하였으며, 기존에 보고된 이산화바나듐 재료와 마찬가지로 약 68도 부근에서 상전이를 일으키는 것을 확인하였다.

이를 제작된 이산화바나듐 나노와이어를 이용하여 저항의 변화가 가능하면서 비휘발성의 특성을 가지는 멤리스터를 제조하였다. 나노와이어의 경우 그 작은 부피로 인해 추가적인 발열체 없이 줄(Joule)열을 이용하여 비휘발성을 확보할 수 있었다. 기존의 보고된 이산화바나듐 박막을 이용한 멤리스터와 달리 가변하는 저항의 범위가 증가하였으며, 저항의 차이도 증가하였다. 이를 통하여 이산화바나듐 나노와이어를 이용한 멤리스터는 비휘발 메모리로 응용이 가능하며, 저전력의 향상된 성능을 가질 수 있다는 것을 증명하였다.

또한 저항의 변화가 가능하면서 비휘발 특성을 가지는 멤리스터를 응용한 가스센서가 개발가능한 지를 확인하는 연구를 수행하였다. 기존 이산

화바나듐을 이용한 가스센서의 경우, 전이전압을 측정하는 방식을 사용하기 때문에 한번의 측정만이 가능하였으나, 멤리스터를 응용한 가스센서는 저항의 변화를 이용하기 때문에 반복적인 측정이 가능하다는 장점을 가진다. 주위의 가스 압력이 감소함에 따라 저항의 감소가 더 커지는 것을 확인하였으며, 변화한 저항이 유지되는 것을 확인하였다. 이를 통하여 멤리스터를 응용한 이산화바나듐 가스센서의 응용가능성을 확인하였다.

마지막으로 이산화바나듐 나노와이어와 폴리머 복합체 형태의 온도가변형 적외선 차단 필름을 제조하였다. MPTMS 처리를 통하여 유기물에 나노와이어가 안정적으로 분산할 수 있도록 하였으며, TEOS를 이용하여 나노와이어 표면을 이산화실리콘으로 감싸줌으로써 광학적 투과도를 높일 수 있었다.

본 연구에서는 순수한 이산화바나듐 나노와이어를 합성하는 공정을 개발하고, 멤리스터, 가스센서, 적외선 차단 소재로서의 응용가능성을 확인하였다. 이산화바나듐 나노와이어를 이용한 멤리스터는 첫번째 보고이며, 자가 발열을 통한 멤리스터 소자 구동 역시 첫번째 보고이다. 기존에 가스센서의 단점을 극복할 수 있는 새로운 형태의 가스센서를 제안하고,

그 가능성을 확인하였다. 또한 제조된 이산화바나듐 나노와이어에 표면 처리를 통하여 그 특성을 향상시킴으로써 실제 이산화바나듐 나노와이어를 이용한 소자 개발에 중요 문제들을 해결 할 수 있는 방법을 제시하였다. 이를 통해 이산화바나듐 나노와이어를 이용한 나노소자 개발에 있어 중요한 기여를 했다고 생각한다.

주요어 : 이산화바나듐, 나노와이어, 나노구조, 수열합성법, 멤리스터, 가스센서, 온도가변형 적외선 차단소재, 자가발열, 비휘발메모리.